FCP Report No. 39

FATIGUE BEHAVIOR AND CRACK DEVELOPMENT IN COMPACTED GRAPHITE CAST IRON

by

Lawrence Molinaro [redacted]
Department of Mechanical and Industrial Engineering

Fatigue properties of compacted graphite cast irons are related to the free graphite configuration. Compacted graphite irons, owing to their intermediary structure, exhibit mechanical properties that lie between those of gray and nodular irons. Two different CG irons were fatigue tested and the resulting variance in their response related to dissimilarities in their graphite morphology.

A Report of the
FRACTURE CONTROL PROGRAM
College of Engineering, University of Illinois
Urbana, Illinois 61801

May, 1981

ACKNOWLEDGEMENT

This investigation was supported by the Fracture Control Program, College of Engineering, University of Illinois at Urbana-Champaign. Tests were conducted in the Materials Engineering Research Laboratory.

Professor Darrell F. Socie is gratefully acknowledged for his counsel which has contributed to the author's professional development. Special gratitude is due Mr. L. L. Fosbinder, Deere and Company, for providing some data on compacted graphite cast iron. Appreciation is also due colleagues James W. Fash and Eric J. Tuegel for their many valuable suggestions and assistance throughout the testing program.

The author is indebted to June Kempka and Amanda Horner for typing the manuscript. Mark Kindig is also thanked for drafting the figures.

TABLE OF CONTENTS

LIST OF TABLES

LIST OF FIGURES

I. INTRODUCTION

A. BACKGROUND

1. Mechanical Behavior of Cast Irons as Related to Graphite Configuration

The effect of graphite configuration on the static and fatigue properties attained in cast irons has been the subject of numerous investigations. As a result of these studies, various trends have been established which relate the graphite morphology of these materials to their mechanical properties. In particular, the relationship of graphite structure to fatigue performance has been of considerable interest on account of the frequent use of cast iron for machine components, where fatigue plays a predominant role in the reduction of useful service life. The performance of a particular cast iron depends on the quantity, size, and shape of the graphite constituent as well as its interaction with the matrix structure.

Cast irons, unlike mild steels, do not exhibit a characteristic yield point. Instead, the curve of plastic deformation merges into the "elastic" portion. Lack of a definite elastic-plastic transition in cast irons is due to the presence of free graphite which modifies the stress distribution within the matrix. These graphite formations can be regarded as inherent notches whose stress concentration varies with effective notch geometry [1]. An increase in notch severity results in a decrease in the tangent modulus, indicating a corresponding increase in plastic deformation.

Fatigue behavior of various cast irons containing different graphite configurations were compared by Ikawa and Ohira [2]. Nodular (ductile) iron exhibited the best fatigue resistance while gray iron displayed relatively poor fatigue properties. The superior peformance of nodular iron over gray iron has been attributed to the dissimilarity in graphite morphology between the two materials. Graphite in gray iron is a highly branched and

interconnected formation within a eutectic cell cluster. These cell structures are composed of sharp flake edges which provide paths of easy fracture in addition to regions of high stress concentration. Nodular iron, on the other hand, contains graphite particles of nearly spherical shape which are non-interconnected, thus minimizing stress concentration effects and interrupting planes of easy fracture. Accordingly, nodular iron exhibits higher strength (both static and fatigue), ductility, and toughness than does gray iron.

In order to better predict the fatigue life of cast iron components in service, a deeper understanding of the mechanism of crack formation and growth in cast irons is required. Gilbert [3,4,5] studied the stress-strain response of these materials in tension and compression and reported the observed mechanism of failure. Under the assumption that the free graphite phase would not transmit a tensile stress, cast iron was modeled as a steel-like matrix containing effective notches of graphite. These graphite particles, when loaded in tension, separate from the matrix interface. Local stresses are produced which exceed the material's cohesive strength under the particular conditions of loading. Cracks were detected at these regions of highly localized stress indicating the significance of graphite in the process of crack initiation in cast irons. Many investigations have subsequently been undertaken to better explain and compare the mechanisms of crack initiation and propagation in both gray and nodular iron.

Fatigue cracks in gray iron have been observed to originate at the graphite flakes [2,6]. Increased graphite flake size results in an increase in notch severity and hence a decrease in the fatigue resistance [2,7]. Initiation of cracks have been detected at rather early stages in the life of gray iron specimens [6]. Under low to medium loading conditions, cracks have

started at flakes most normally oriented to the loading axis, resulting in the extensive development of only a few major crack systems. At higher loading situations, cracks were observed to originate from flakes oriented randomly as well as normal to the direction of loading. The development of more numerous crack systems occurred in the latter case. On the basis of these observations, the early crack growth process in gray iron appears to be dominated by the size and orientation of graphite flakes.

The controlling mechanism for crack initiation in nodular iron is not as well defined as that in gray iron. Graphite nodules, under a tensile load, have been demonstrated to debond from the surrounding matrix [4]. The initiation of cracks from the resulting weak boundaries has been observed by Mitchell [8]. Other investigations have shown that fatigue cracks initiate from not only nodules but also from casting imperfections such as inclusions, microshrinkage pores, and irregularly shaped graphite clusters [9,10]. These irregularities have been determined to initiate cracks at an earlier stage in life than well formed nodules. This result is not surprising due to the irregular size and shape of these casting discontinuities which increase the severity of stress concentration. Whatever the initiation process, these cracks have been detected rather early in the life of nodular iron specimens [10].

Once initiated, cracks in both gray and nodular irons propagate by merging or linking up with other cracks, graphite structures, and discontinuities. Previous studies have reported up to 95 percent of the fatigue lifetime of cast irons being spent in crack growth [6,10]. This observation implies that the use of a crack initiation model to account for the accumulation of damage in cast irons [8], while sufficient for constant amplitude loading, may be inadequate for the variable amplitude case.

A type of cast iron with graphite configuration intermediate to that of gray and nodular iron has recently received increased attention for engineering use because of its fine mixture of mechanical, thermal, and casting properties. This intermediary form, referred to as compacted graphite iron, can be achieved by the variation of such factors as section size, rate of cooling and chemical composition. The historical development of compacted graphite cast iron as well as its mechanical properties and current methods of production will be explored in greater detail in the course of this introductory chapter.

2. Development and History of Compacted Graphite Cast Iron

Compacted graphite (CG) iron is a type of cast iron possessing a graphite configuration intermediate to that of the conventional gray and nodular irons. Although its existence has been known for years, this material had not been utilized on a large scale due to certain practical difficulties in its production.

Morrogh [11] referred to compacted graphite in 1948, the preparation of which was unintentionally accomplished as a result of investigations into the production of nodular cast iron by cerium (Ce) treatment. When a sufficient amount of Ce was added to hypereutectic irons, configurations of completely developed nodular graphite resulted. Yet, when hypoeutectic irons were treated with Ce, a graphite structure was obtained which appeared as a short, thick variation of the normal form of flake found in gray iron. Hence, these structures were referred to as quasi-flake graphite. Practical application of this intermediate form of cast iron was overshadowed by the production and use of the stronger, more ductile nodular irons.

The production of nodular iron by Ce treatment was soon replaced by processes employing magnesium (Mg) as the major effective additive. Addition of Mg resulted in easier production of nodular graphite in hypoeutectic as well as hypereutectic irons. However, when the residual Mg content of the iron was below that necessary to acquire nodular graphite formation, compacted graphite was once again observed to form. Production of compacted graphite irons by this process requires the close control of Mg content within extremely narrow limits. Too little Mg fails to produce fully compacted graphite configurations while over-treatment results in the development of nodular graphite. The margin of error between under- and over-treatment can be as sensitive as 0.005 percent Mg [12], making the generation of CG iron impractical in light of the easier production of nodular irons.

Despite its lack of commercial use, this intermediate form of cast iron continued to appear in technical literature under a variety of names. The graphite structure has been referred to as up-graded, semi-nodular, quasi-flake, compacted flake, floccular and vermicular in addition to the now generally accepted term "compacted graphite." Various alternative methods of production have arisen in the years following the accidental development of these irons.

Gilbert [13] achieved an intermediate form of graphite by a procedure consisting of strong desulfurization ($S < 0.002$ percent) and rapid solidification in the mold. Desulfurization was accomplished by the introduction of calcium to the molten iron. The fine worm-like shaped graphite resulting from this process appears quite different from the compacted graphite produced by other methods. Vermicular graphite, as this configuration has come to be termed, exhibits little if any interconnection thus raising some controversy over whether this alternate structure may truly be regarded as compacted graphite.

Compacted graphite forms have also been achieved in irons retaining a sufficiently high nitrogen (N_2) content. Dawson, et al. [14] first observed that the presence of N_2 could significantly alter the graphite configuration in cast iron. Compacted graphite structures were readily produced by N_2 existence in irons of medium to heavy section size, whereas the effect was minimal in thinner castings. This technique of using N_2 as an alloying element to produce compacted graphite is rarely employed, however, because of the extreme difficulty of controlling N_2 contents and the risk of forming blowholes in high nitrogen iron castings.

The use of certain minor alloying elements which tend to suppress the formation of nodular graphite has made the production of compacted graphite iron more economically feasible. Schelleng [15] patented a process of attaining CG irons with Mg contents ranging from 0.005 to 0.06 percent. The addition of titanium (Ti) and a rare earth metal made this process possible. Production of compacted graphite by simultaneous treatment of cast iron with spheroidizing and anti-spheroidizing elements have been presented by Sofroni, et al. [16]. In this case, the addition of both Ti and Al were made to the molten iron in order to counteract the strong spheroidizing influence of Mg treatment. As a result of these investigations, a much broader Mg content could be tolerated resulting in the possibility of practical commercial development of compacted graphite iron.

Extensive studies on the reliable production of high duty CG iron were conducted by Aleksandrov, et al. [17]. A production technique involving the treatment of the liquid iron with a complex master alloy composed of rare earth metals and yttrium was developed. The master alloy can be added directly in the furnace crucible, on the ladle floor, or through the tapping stream. Compacted graphite irons were demonstrated to be producible with a reasonable amount of quality control.

Compacted graphite iron has currently become desirable for commercial usage. By means of an excellent mixture of mechanical, thermal, and casting properties, this material makes a promising substitute for conventional cast irons, especially in cases were both high strength and thermal conductivity is required. The advantages of using compacted graphite iron are discussed in greater detail in the following section.

3. Advantages of Compacted Graphite Use

Compacted graphite irons, owing to their intermediate structure, exhibit physical properties that lie between those of gray and nodular irons. The tensile and yield strengths of CG irons approach those of nodular irons while far surpassing those of gray irons. Yet, the thermal conductivity, resistance to thermal shock, and machinability of these irons are more similar to gray rather than nodular irons. Compacted graphite irons are also less susceptible to the development of casting problems normally associated with nodular iron production. The commercial utilization of compacted graphite iron appears imminent because of its splendid combination of physical and casting properties coupled with the recent development of production methods furnishing improved quality control. In order to gain a better appreciation of its potential, the advantages of CG iron usage will be more thoroughly discussed.

The graphite in cast iron has a much higher thermal conductivity than the metallic matrix. It follows that the amount, configuration, and distribution of the graphite phase controls the thermal conductivity achieved in a particular cast iron. The coarse, interconnected flake form in gray iron imparts a high thermal conductivity, whereas the discrete spheroidal structure furnishes nodular iron with a comparatively low thermal conductivity [18].

The interconnected, blunt, flake-like structure of compacted graphite imparts a thermal conductivity similar to, although slightly less than gray iron [19].

The tensile strength of compacted graphite iron is less sensitive to variations of carbon equivalent than that of gray iron [20]. The strength (both ultimate and yield) and elongation at failure of CG iron are significantly greater than those achieved in gray iron [19,20]. In light of these superior mechanical properties, compacted graphite iron seems a promising replacement for gray cast iron as a load-carrying material capable of withstanding increased strength, ductility, and toughness requirements.

The fluidity of cast iron is controlled by the carbon equivalent of the iron [18]. Therefore, all cast irons of like carbon equivalent will exhibit, in the molten state, similar abilities to fill a mold cavity. However, in order to obtain increased strengths, gray irons are produced at low carbon equivalent contents. Compacted graphite irons with high carbon equivalents have strengths at least equal to those of even the highest duty gray iron [12]. Likewise, compacted graphite irons have greater fluidity than gray irons of equivalent tensile strengths.

The machinability of cast irons varies inversely with the mechanical properties. Improved machinability is generally associated with low strengths, hardnesses and ductilities [18]. Consequently, compacted graphite irons are more easily machined than nodular irons.

Compacted graphite irons are less apt to develop certain casting difficulties commonly come across during the production of nodular iron castings [12]. One such problem is the formation of dross on the surface of molten iron. Accumulation occurs largely because of oxidation but also due to the rising of impurities to the surface. This dilemma is less frequently

encountered with CG production. Nodular iron, because of its mode of solidification, requires more extensive feed metal than gray iron [18]. A large quantity of molten metal must be provided to the region undergoing solidification at a rate sufficient to fill the mold cavity ahead of the advancing solidification front. Compensation for any shrinkage accompanying soldification must be made as well. Feeding requirements of compacted graphite iron, although greater than those of gray iron, are much less than those of nodular [12]. That being the case, compacted graphite castings are less susceptible to the formation of shrinkage cavities than those made of nodular iron.

Compacted graphite irons appear to be particularly well suited for components subjected to wide-ranging temperature variations, where the combination of the excellent mechanical properties of nodular iron along with the castability and thermal conductivity associated with gray iron are desired. These irons have recently been selected for use in electric motor casings and bedplates [19]. Very good casting quality was achieved with no defects or shrinkage observed.

4. Variation of Compacted Graphite Configuration and Properties

The graphite flake structure in gray iron can be altered, by methods stated previously, to obtain a compacted graphite configuration. This modification process involves the blunting of graphite flake edges followed by a general thickening and shortening of these flakes. Depending on the production technique and extent of graphite compaction, various modifications of compacted graphite itself may result. Riposan and Sofroni [21] classified compacted graphite size and shape into three typical forms in accordance with Table 1. The size, degree of interconnection, and length-to-thickness ratio

of the graphite phase were found to influence the mechanical behavior acquired.

The presence of graphite structures approaching a spherical or nodular shape will also effect the physical behavior of CG irons. Aleksandrov, et al. [19] illustrated that as the percentage of nodular configuration was increased, mechanical properties such as tensile strength and elongation were enhanced. Similar improvements were also noted with respect to fatigue and impact resistance. By variation of processing conditions, cast iron consisting of compacted and nodular graphite (up to 90 percent) may be readily produced. Depending on the combination of properties desired, optimum compacted-nodular joint structures can be developed. An excellent merger of mechanical, thermal, and casting properties was obtained with a compacted graphite iron containing approximately 30 percent nodular graphite [19].

B. Purpose and Scope of Investigation

This investigation involves the observation of fatigue crack initiation and growth in compacted graphite iron. A procedure of replicating the specimen surface at designated intervals throughout its life is employed. Formation and development of crack systems is monitored in order to identify the mechanism of early crack growth. A comparison is then made with gray iron, whose crack initiation and growth were examined in a previous study [6]. The purpose of this investigation is to obtain an improved comprehension of this crack development mechanism in order to better predict the fatigue performance of potential CG components in service.

Crack growth data of compacted graphite under fully reversed load control has been obtained. The strain amplitude during these cyclic tests has been monitored and is shown to correlate well with crack growth. A continually

increasing strain amplitude is observed and this trend is inferred to be a result of developing cracks.

The fatigue test results from both compacted graphite and gray iron are presented and the superior performance of the former exhibited. Two different compacted graphite irons are also tested and the variance in their properties related to dissimilarities in their graphite structure.

II. EXPERIMENTAL PROGRAM

A. Material Description

The materials used in this investigaton were provided by Deere and Company, Moline, Illinois. In addition, they provided experimental data on another compacted graphite iron, designated CG(B), for comparison purposes. The matrix structure of all cast irons tested consisted primarily of pearlite. In order to achieve this pearlitic matrix, 30 mm in diameter by 200 mm in length test bars were sand cast in green molds and then air cooled through the critical austenite transformation range (720 to 900°C).

Two variations of compacted graphite were produced. In each case, compacted graphite configuration was accomplished by the simultaneous treatment of the molten iron with Mg (as a spheroidizing element) in addition to Ti and Al (as anti-spheroidizing elements). Hence, both of these CG irons can be grouped under the general classification of Type III according to Table 1. Upon examination of the microstructures of these irons (Figs. 1 and 2), an obvious dissimilarity is apparent. The iron designated as CG(A) contains significantly less spheroidal shaped graphite than that which can be observed in iron CG(B). This difference is due chiefly to the presence of three times the Ti content in CG(A) as compared to CG(B). Titanium helps suppress the formation of spherically shaped graphite, and thus serves to counteract the spheroidizing influence of Mg. As previously mentioned, the actual percentage of nodular shaped graphite in CG irons can influence the mechanical properties obtained. This effect will be more fully discussed later in this investigation.

A pearlitic gray iron, whose fatigue performance has been a subject of a previous study [6], is included in this research as a means of comparison with the compacted graphite irons. The matrix and flake structure of this iron is

shown in Fig. 3. Material compositions for all three irons are presented in Table 2.

B. Specimen Preparation

Smooth, cylindrical specimens were machined from the as-cast test bars. The dimensions for these specimens are given in Fig. 4. A standard surface finish, as specified by ASTM E606, was attained for each test specimen. This degree of finish was sufficient for monotonic and base-line fatigue tests, however, a finer polish was required in order to obtain a clear resolution for crack growth observations. These specimens, while being rotated on a lathe, were mechanically polished with a pneumatic rotary polishing rod wrapped with separate strips of emery paper and felt. Initial rough polishing was accomplished with the emery paper, followed by a fine polishing procedure utilizing the felt saturated with a suspension of 0.3 micron alumina metallographic powder in water. An acceptable surface finish was obtained once machining and rough polishing marks were almost completely eliminated.

C. Test System

Material testing performed during the course of this investigation was accomplished in the Materials Engineering Research Laboratory at the University of Illinois at Urbana-Champaign. An MTS computer-based materials test system was employed for the performance of all tests. This system consists of a $\pm$20-kip closed loop servohydraulic test frame interfaced with a multiuser digital minicomputer, CRT graphics display terminal, and a hard-copy unit. Function generation, data acquisition, and data analysis were implemented through MTS BASIC, a modified version of the interactive BASIC programming language.

D. Testing Procedures

1. Monotonic Tests

Monotonic tension and compression tests were performed on both compacted graphite irons. An axial extensometer was used to monitor and record the monotonic response. All test were software controlled and the resulting stress-strain data was digitized and stored on floppy disks.

2. Cyclic Tests

a. Strain-Controlled

Constant amplitude, completely reversed, strain-controlled axial fatigue tests were executed at five different strain amplitudes for each of the compacted graphite irons. Three specimens were tested to failure at each amplitude of strain. An axial extensometer was used to monitor and record the cyclic response. All tests were software controlled and the resulting hysteresis loops were digitally recorded at every power of two cycles. Fatigue failure was defined as 90 percent load decay from the initial maximum tensile load.

b. Load-Controlled

Constant amplitude, completely reversed, load-controlled axial fatigue tests were performed on the compacted graphite iron designated as CG(A) and on the pearlitic gray iron. Each iron was tested at five different stress amplitudes, with approximately three specimens tested at each amplitude. An axial extensometer was used to monitor and record cyclic response. Software control was implemented to obtain base-line data while manual analog control was used for the performance of crack growth observation

tests. Fatigue failure was defined, in this case, as the complete separation of the smooth specimens into two pieces.

3. Crack Growth Observation Tests

a. Purpose of Replication

An improved understanding of the mechanism of early crack growth in cast irons is necessary to adequately predict the fatigue performance of these materials in service. Toward this goal, a procedure was developed which makes possible the observation of crack initiation and progression on the entire surface of axially loaded smooth specimens. This technique, termed replicating, has previously been used to successfully monitor the development of crack systems in both gray and nodular irons [6,10]. Quantitative crack growth data may be obtained from the resulting fatigue life history. In addition, the amount and extent of crack development can be qualitatively observed at various stages throughout the life.

b. Replication Procedure

A replicating procedure was adopted in this investigation to monitor fatigue crack formation and growth in both gray and compacted graphite iron. As previously described, all specimens used for replicating were subjected to a fine polishing treatment prior to testing. Once the proper finish was attained, the surface of each specimen was divided into three distinct regions. This apportionment was required to insure total coverage of the gage section, a necessity, since the origin of a crack cannot be predetermined before testing. Acetyl cellulose film (0.034 mm thick) was employed to obtain a reproduction of the specimen surface. This film was cut into tape-like strips of width approximately equal to the specimen gage length.

A replica was obtained by the injection of acetone via syringe into the pocket formed between the specimen surface and a strip of film held loosely around this surface. Immediately following injection, the film was pulled taut against the specimen which resulted in the spreading of acetone over the entire region of interest. The acetyl cellulose tape, softened on initial contact with acetone, adhered to the specimen surface. The film was then left undisturbed for approximately two minutes, during which simultaneous evaporation of acetone and hardening of the replicating tape had occurred. At this stage, the film had become an exact representation of the surface it is in contact with. The finished replica can then be removed from the specimen and quickly placed between two microscope slides. This procedure was repeated six times, twice at each of the three regions, during each interval in the life of a specimen. Each replicating session, composed of six individual replications, constitutes a total surface replica representing the entire gage section at one particular point in its life.

Surface replicas were taken at approximately every 10 percent of a specimen's expected life which was estimated from the results of base-line data. Peak strain amplitude was monitored during these load-controlled replication tests. If an increase of about 8 percent in strain amplitude was observed prior to the expected 10 percent increment in life, a series of replicas were obtained in order to detect the source of strain increase. The procedure for obtaining replicas in load control mode is outlined in the APPENDIX.

c. Observation of Replicas

Observation of the finished replicas was accomplished with the aid of an optical microscope. The major crack system, defined as the largest crack system present near failure, was located and photographed using a polaroid camera attachment. Good contrast was achieved while transmitting light up through the replicas. Development of the failure crack system could then be recorded by tracing backwards from the photograph depicting the crack near failure to replicas taken at successively earlier stages in the fatigue life. Quantitative crack length data at each respective interval in the life was obtained in this manner.

III. EXPERIMENTAL RESULTS

A. Monotonic

Monotonic tension properties of the two compacted graphite irons and the pearlitic gray iron are given in Table 3. Figures 5, 6, and 7 illustrate the monotonic stress-strain response of these three materials. The monotonic properties and stress-strain curve for gray iron were obtained from a previous investigation [6].

B. Fatigue

Table 4 summarizes the outcome of completely reversed load-controlled tests for compacted graphite iron CG(A). Results from similar tests performed on the pearlitic gray iron are presented in Table 5. Stress-life data from both of these materials is plotted in Fig. 8. This data comprises the results of base-line and crack growth observation tests.

The results of completely reversed strain-controlled tests for compacted graphite irons CG(A) and CG(B) are given in Tables 6 and 7. Strain-life data for these two CG irons is plotted in Fig. 9. Figures 10 and 11 include strain-life data from the pearlitic gray iron for the purpose of comparison with CG(A) and CG(B), respectively. Strain-life data for all three cast irons is plotted in Fig. 12 and their respective curves shown in Fig. 13.

Representative hysteresis response for CG(A) and pearlitic gray iron tested under load-controlled conditions is shown in Figs. 14 through 17. The peak strain amplitude rises continuously and stable response is never attained. Therefore, a cyclic stress-strain curve is not presented.

C. Crack Growth

Crack formation and growth in compacted graphite and gray iron has been monitored by means of the cellulose acetate replicating procedure previously described. Examination of the finished surface replicas resulted in the detection of the major (failure) crack system(s). Once identified, each crack system was reproduced as a composite photographic history of crack progression. A representative example of such a crack development record is shown in Fig. 18.

The crack length at any given stage in the life was taken as the distance of the largest portion of the failure crack system. If two or more well developed crack groups were observed to be overlapping or nearly connecting, the sum of their lengths was considered as the total crack distance at that particular phase in the fatigue life. Crack length versus applied cycles data for compacted graphite CG(A) and pearlitic gray iron tested under load control mode is presented in Figs. 19 and 20, respectively. Each curve on these plots represents the crack growth at one particular value of stress amplitude.

The maximum strain amplitude was also monitored throughout all load-controlled replicating tests. A continuous increase in this peak strain amplitude was observed in every test case. This strain rise trend is illustrated in Figs. 21 and 22 for the materials CG(A) and pearlitic gray iron. The significance of this occurrence and its correlation with the crack growth data is discussed in the subsequent section of this investigation.

IV. DISCUSSION

A. Monotonic Behavior

The monotonic properties of the three cast irons, presented in Table 3, illustrate the relation of mechanical behavior obtained in these materials to their graphite configuration. Both compacted graphite forms exhibited significantly greater yield and ultimate strengths as well as more ductility than that of the gray iron. These superior properties have been attributed to the presence of blunted graphite particles in compacted graphite which provide a less severe stress concentration under a tensile load than the sharp-tipped flake counterpart in gray iron.

The disparity in mechanical properties displayed by the two compacted graphite irons resulted from the contrast in the percentage of nodular shaped graphite existing within their matrix. Type CG(B) possesses nearly five times the amount of spherically shaped graphite as that observed in CG(A) iron (Figs. 1 and 2). Such an increase in the percentage of high nodularity graphite has been found to enhance the mechanical properties obtained [19]. It follows that the compacted graphite iron designated CG(B) would exhibit superior monotonic properties when compared with CG(A) iron. The results of monotonic tests performed on these two materials support this general trend.

Monotonic tensile stress-strain behavior for the three irons (Figs. 5, 6, and 7) exemplify the characteristic anelastic response of cast irons. These materials do not exhibit a definite yield point phenomenon. The presence of free graphite phase modifies the stress distribution within the matrix and results in plastic yielding at low nominal stress levels. Therefore, the curve of plastic deformation is seen to merge directly into the elastic portion.

B. Fatigue Behavior

The fatigue response of compacted graphite iron in both strain- and load-control has been observed and the results of these tests have been presented. Two types of CG iron were studied and any variation in their fatigue behavior will be discussed. A comparison will also be made with the response of a pearlitic gray iron under both control modes. The fatigue behavior of these cast irons will then be discussed in relation to the form of the free graphite constituent present in their respective microstructures.

Compacted graphite iron, Type CG(A), performed extremely well under a fully reversed load-controlled testing situation relative to gray iron response under similar loading conditions. The superiority of CG(A) iron in this fatigue situation is illustrated by Fig. 8. A considerably lower stress amplitude was sufficient in gray iron to produce comparable fatigue life values as those attained by much more highly stressed compacted graphite specimens. Lives approaching 1×10^6 cycles were encountered in CG(A) specimens at a stress amplitude of 160 (MPa) whereas gray iron at this same stress amplitude failed at approximately 200 cycles. The CG iron exhibited a fatigue limit at nearly twice the stress amplitude as that observed in the gray iron.

Compacted graphite iron CG(B) exhibited better fatigue resistance than CG(A) under strain-controlled conditions. The strain-life plot of these two CG irons (Fig. 9) illustrates this contrast in fatigue performance. At each strain-amplitude, CG(B) iron displayed a fatigue life nearly three times greater than that attained by CG(A) iron. As previously indicated, cast iron CG(B) contains approximately five times the amount of nodular shaped graphite as does CG(A) iron. This result supports the findings of prior investigations concerning the enhancement of mechancial properties achieved in compacted

graphite irons containing increasing percentages of nodular shaped graphite [19].

Compacted graphite iron specimens generally exhibited better fatigue response than did gray iron specimens, as shown by Figs. 10 through 13. In particular, CG(B) iron was superior to the gray iron in strain-controlled testing. This iron achieved fatigue lives that were nearly an order of magnitude greater than gray iron lives at the same strain amplitude. Compacted graphite iron CG(A) also attained fatigue response that was better than gray iron, although not to the same degree as CG(B).

The results of fatigue tests performed on these three cast irons are consistent with the observations of previous investigations. The morphology of the free graphite constituent appears to significantly influence the response to cyclic loading for these materials. Compacted graphite irons, with their blunted particle ends, are seen to perform much better in fatigue than gray irons, which contain sharp-tipped graphite flakes. The presence of spherically shaped or nodular graphite in CG irons is seen to improve the fatigue resistance of these materials.

C. Crack Growth Behavior

1. Qualitative Observations

Observation of crack formation and growth in cast irons has been accomplished by optically scanning surface replicas at intervals throughout the fatigue life. Crack histories were compiled for each specimen at its respective amplitude of loading. Upon careful examination of these histories, qualitative features of fatigue crack development were noted. The origin and relative extent of development of cracks in both CG(A) and gray iron was observed at various stress amplitudes.

Cracks were seen to originate at the graphite microdiscontinuities which induce the most severe stress concentration. Graphite flakes, with their interconnected structure and sharp edges, were observed to initiate cracks in the pearlitic gray iron. This observation was consistent with that of a previous investigation conducted on this material [6]. The formation of cracks in compacted graphite iron generally appeared to start at the modified flake form, however, irregularly shaped graphite particles were also seen to initiate cracks to a lesser degree. Once initiated, these cracks develop via a combination of crack propagation through the matrix material and incremental crack extension brought about by the merging of crack systems.

The extent of crack development in both irons varied with the degree of applied stress. At large stress amplitudes, cracks were detected within the first 5 percent of the fatigue life for both CG(A) and gray iron. Cracks were seen to initiate at several graphite sites oriented both oblique and normal to the loading axis. Many cracks of similar size developed throughout the duration of these high stress-amplitude tests. Several of these cracks were observed to have developed to a significant magnitude, 2 mm and above, near failure of the specimen. Conversely, at low stress amplitudes, cracks were observed to initiate at graphite structures oriented normal to the loading direction. In this case, cracks were detected within the first 10 percent of the specimen life. Although small cracks were found throughout the specimen surface, very few major crack systems were developed near failure. This result is again consistent with gray iron observations.

Crack arrest has been seen to occur in gray irons when cracks join with flake configurations oriented parallel to the loading axis. This sort of crack-tip blunting was also observed to take place in CG(A) iron when cracks encounter spherically or irregularly shaped graphite forms. Since crack

initiation was detected early in the lives of both CG(A) and gray iron, this blunting phenomenon and its relative degree of effectiveness in these two materials may very well influence the rate of crack growth and consequently the fatigue life obtained.

2. Quantitative Observations

a. Crack Growth Rate

Crack length versus applied cycles curves (Figs. 19 and 20) for CG(A) and gray iron indicate that 90 to 95 percent of the specimen life is spent in crack growth. This being the case, an adequate prediction technique of fatigue resistance for both of these cast irons necessitates the use of a crack propagation model. Growth of cracks proceed steadily until they reach the significant size range of 1 to 2 mm at which point rapid growth occurs. Failure ensues at a relatively short number of cycles thereafter.

The rate of crack growth, as indicated by the slopes of the crack growth curves, was seen to vary with the stress level at which testing was performed. Crack length versus normalized cycles (cycles/cycles to failure), shown for both materials in Figs. 23 and 24, illustrates the increase in crack growth rate at successively larger stress amplitudes. This trend was observed in both CG(A) iron and pearlitic gray iron.

At stress amplitudes resulting in similar lives, the slopes of the crack growth curves for gray iron (Fig. 20) are seen to be larger than their counterparts for CG(A) iron (Fig. 19). Ergo, it may be inferred that the crack growth rate of gray iron is larger than that of CG(A) iron at comparable lives. This presumption results in some rather interesting implications pertaining to the relationship between graphite configuration and the mechanism of early crack growth.

Cracks have been observed to initiate at very early stages in the life (approximately 5 to 10 percent) of both CG and gray iron specimens. Thus, it appears that the fatigue resistance of these materials is a function of the crack propagation rather than the initiation process. As previously mentioned, the occurrence of crack-tip blunting was detected in both CG(A) and gray iron. However, the blunted, modified flake form and variable percentage of nodular graphite contained in compacted graphite iron provides a higher probability of encounter between a growing crack and a potential crack-arrester. Therefore, one would expect crack growth in CG iron to progress at a slower rate than gray iron until a crack system(s) reaches the critical size range (1 to 2 mm) after which crack growth proceeds rapidly to failure. This hypothesis appears consistent with the results of the crack growth data discussed above.

b. Strain Extension

The maximum strain amplitude attained at each successive cycle during load-controlled fatigue tests has been observed to increase continuously for both CG(A) and gray iron. The rate of strain rise which is related to the slope of the strain amplitude versus cycles curves was found to vary with the stress amplitude at which the test was conducted. As illustrated in Figs. 21 and 22, this strain rise rate increased at successively larger stress amplitudes in both materials. This trend is consistent with the load drop phenomenon reported in a previous study of gray iron under strain-controlled test conditions [6].

A comparison of the strain extension response of the two cast irons reveals an interesting feature. At stress amplitudes producing comparable fatigue lives, the slopes of the strain rise curves for gray iron (Fig. 22)

are seen to be greater than those for CG(A) iron (Fig. 21). Since the slopes of these strain extension curves provide an indication of the strain rates, it is inferred that the rate of strain rise of gray iron is larger than that of CG(A) under load-controlled conditions.

Tucker and Olberts [22] have reported cyclic softening behavior in cast iron specimens which would definitely result in an increase in the peak strain values during load-controlled tests. However, the effect of cyclic softening would be a rapid initial increase in strain amplitude with stabilization occurring at approximately 50 percent of the fatigue life. The shape of the strain extension curves and the fact that the strain amplitude did not stabilize at any point in the life indicate that this strain rise trend was not a result of cyclic softening. Rather, it is suspected that this extension of strain amplitude was due to crack formation.

c. Relation of Strain Extension to Crack Growth

Strain extension trends have been observed to vary with applied stress amplitude in a manner consistent with the corresponding crack growth trends. At large stress amplitudes, both the strain rise and crack growth rates, as inferred from the slopes of their respective curves, are larger than at smaller amplitudes. Figures 25 through 28 illustrate the relationship of strain extension to crack growth curves for representative CG and gray iron specimens. These normalized crack length and strain amplitude versus life curves exhibit compatible trends. It is therefore concluded that the strain extension phenomenon observed in load-controlled tests for CG and gray iron results from the accumulation of damage in the form of developing crack systems.

V. CONCLUSIONS

The monotonic and fatigue response of two compacted graphite variations was studied. Superiority of the mechanical properties attained by one CG iron over the other was attributed to the differences in their graphite configuration. Strain- and stress-life fatigue data for the compacted graphite irons was better than that obtained from a pearlitic gray iron.

The formation and growth of fatigue cracks has been monitored for compacted graphite iron. Detection of cracks very early in the life (approximately 5 to 10 percent) illustrated that the majority of fatigue life was expended in crack growth. Similar observations for a pearlitic gray iron indicated the significance of propagation rather than initiation processes in the disparate fatigue response of these two materials.

A continuous strain rise was observed during load controlled fatigue tests for both CG and gray iron. This phenomenon has been shown to relate well with the development of crack systems. Crack growth and strain extension rates were seen to increase at successively larger stress amplitudes. These rates were observed to be greater in pearlitic gray than in compacted graphite iron. The higher potential for crack-tip blunting to occur in CG over gray iron was postulated as a plausible explanation for this result.

Compacted graphite iron, with its spendid combination of physical and casting properties, makes a promising substitute for conventional cast irons in cases where both high fatigue strength and thermal conductivity is required. A better comprehension of the crack development process in these materials should result in improved life prediction of potential CG cast components in service.

VI. SUGGESTIONS FOR FURTHER STUDY

The variation of mechanical properties attained by the two compacted graphite irons was inferred to be a result of differences in their graphite structure. However, the presence of unusual defects or other casting imperfections would also account for the observed discrepancies in monotonic and fatigue response. A thorough examination of the representative casting qualities via scanning electron microscopy is suggested.

Strain-controlled replicating tests should be conducted on the compacted graphite iron. The peak stress amplitude could be monitored and the resulting load drop related to the development of cracks. Results could then be compared with those of gray iron under the same test conditions. Observation of the development of fatigue cracks in nodular iron via replicating procedure would be valuable to the understanding of early crack growth mechanism in cast iron materials. The response of all three irons under variable amplitude loading could then be studied with the ultimate goal of improved life prediction techniques for cast iron components in service.

Table 1 Typical Forms of Compacted Graphite and Corresponding Properties Obtained [21]

	Graphite Dimensions			Properties Obtained			
Graphite Type	Length L_{max} (μm)	Thickness d_{max} (μm)	L/d	Tensile Strength (MPa)	Yield Strength (%)	Brinell Hardness	Methods of Manufacture
I	20	10	2-4	300-450	2-5	150-240	Strong desulfurization, especially with Ca (S<0.002%)
II	150	50	2-5	350-500	3-9	150-240	Treatment of the liquid iron with Ce and rare earth metals
III	150	20	3-10	300-450	1-3.5	150-250	Treatment with Mg and addition of Ti, Al, or Sb

Table 2 Material Compositions

	C	Si	Mn	P	S	Cr	Ni	Mo	Cu	Mg	Ti	Sn	Al
CG(A)	3.60	2.40	0.48	0.01	0.01	0.05	0.48	0.01	0.28	0.02	0.18	0.10	0.01
CG(B)	3.50	2.48	0.70	0.01	0.015	0.03	0.05	-	0.81	0.02	0.06	0.01	0.02
Pearlitic Gray Iron	3.30	2.20	0.44	0.01	0.02	0.03	0.06	0.01	0.40	-	0.01	-	0.01

Table 3 Mechanical Properties

	CG(A)	CG(B)	Pearlitic Gray Iron
Modulus of Elasticity E (Tension) GPa	134	140	84
Yield Strength 0.2% Sy MPa	345	420	185
Ultimate Strength True Fracture Strength, σ_f MPa	438	570	228
True Fracture Ductility ε_f	0.0153	0.0308	0.0122
Bulk Hardness (3000 kg)	195	215	180

Table 4 Stress-Life Data for Completely Reversed Load Controlled Tests CG(A)

Specimen No.	Total Load Amplitude $\Delta P/2$ (KN)	Total Stress Amplitude σ_a (MPa)	Cycles to Failure N_f
CG-126	23.6	300	137*
CG-22	23.6	300	156
CG-8	23.6	300	178*
CG-9	17.7	225	1,968*
CG-121	17.7	225	2,062*
CG-27	17.7	225	5,858.5
CG-23	17.7	225	8,954.5
CG-5	14.9	190	11,492*
CG-25	14.9	190	28,079.5
CG-24	14.9	190	33,053
CG-122	14.9	190	42,118*
CG-124	13.3	170	54,821*
CG-13	13.3	170	65,824.5
CG-100	13.3	170	71,980*
CG-6	13.3	170	117,669
CG-105	12.6	160	788,756*
CG-26	12.6	160	880,529

* Crack Growth Test

Table 5 Stress-Life Data for Completely Reversed Load Controlled Tests Pearlitic Gray Iron

Specimen No.	Total Load Amplitude $\Delta P/2$ (kN)	Total Stress Amplitude σ_a (MPa)	Cycles to Failure N_f
CI-200	12.6	160	259
CI-209	11.0	140	526*
CI-201	11.0	140	764.5
CI-206	9.4	120	2,425*
CI-202	9.4	120	3,310
CI-207	9.4	120	4,728*
CI-208	7.9	100	8,174*
CI-203	7.9	100	15,787
CI-204	7.9	100	23,025
CI-210	7.1	90	28,422*
CI-211	7.1	90	37,951*
CI-212	6.7	85	65,798*
CI-213	6.7	85	109,550*

*Crack Growth Test

Table 6 Strain-Life Data for Completely Reversed Strain Controlled Tests CG(A)

Specimen No.	Total Strain Amplitude $\Delta\varepsilon/2$	Maximum Average Stress Amplitude σ_{max} (MPa)	Cycles to Failure N_f
C-2	0.001	130.6	700,989
C-3	0.001	127.0	569,727
C-12	0.001	139.0	208,742
C-7	0.0015	186.6	39,842
C-9	0.0015	178.2	112,370
C-8	0.0015	181.6	157,210
C-16	0.0015	185.0	239,215
C-1	0.002	224.2	16,074.5
C-5	0.002	233.3	4,011.5
C-4	0.003	297.5	799.5
C-6	0.003	298.6	1,205.5
C-10	0.003	236.1	6,839
C-11	0.003	293.0	921.5
C-13	0.004	394.4	199.5
C-14	0.004	320.9	311

Table 7 Strain-Life Data for Completely Reversed Strain Controlled Tests CG(B)

Specimen No.	Total Strain Amplitude $\Delta\varepsilon/2$	Maximum Average Stress Amplitude $\bar{\sigma}_{max}$ (MPa)	Cycles to Failure N_f
13	0.0015	211.5	1.04×10^6
14	0.0015	210.9	714,332
15	0.0015	208.5	949,248
4	0.002	273.1	41,700
10	0.002	273.1	26,197
11	0.002	269.8	24,900
1	0.003	325.8	5,158
2	0.003	335.4	2,965
5	0.003	325.0	2,226
3	0.004	370.0	725
6	0.004	368.1	559
7	0.004	368.9	686
8	0.005	404.9	205
9	0.005	393.1	265
12	0.005	390.6	339

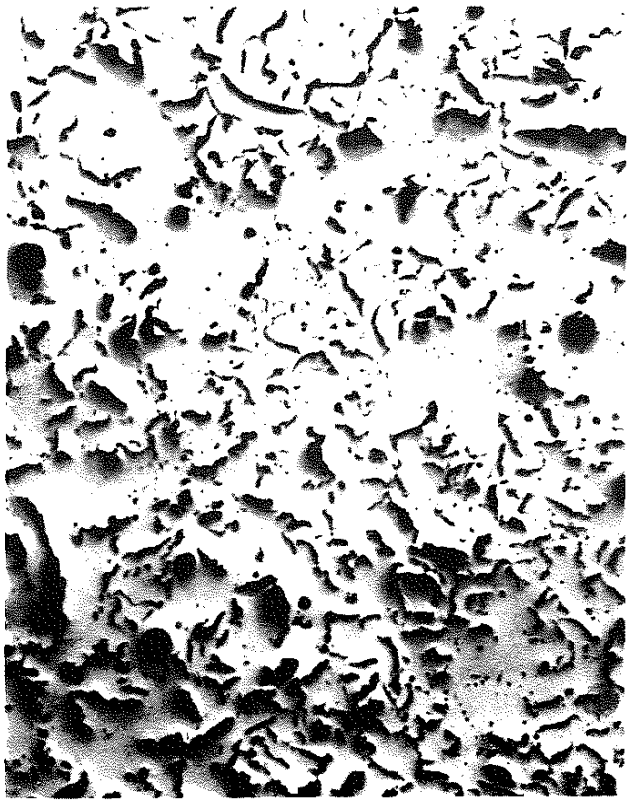

(i)

(ii)

Figure 1 Compacted Graphite Iron-CG(A)
(i) CG Form with ≈5% Nodular Graphite
(ii) Matrix Microstructure-Pearlite Etched 2% Nital

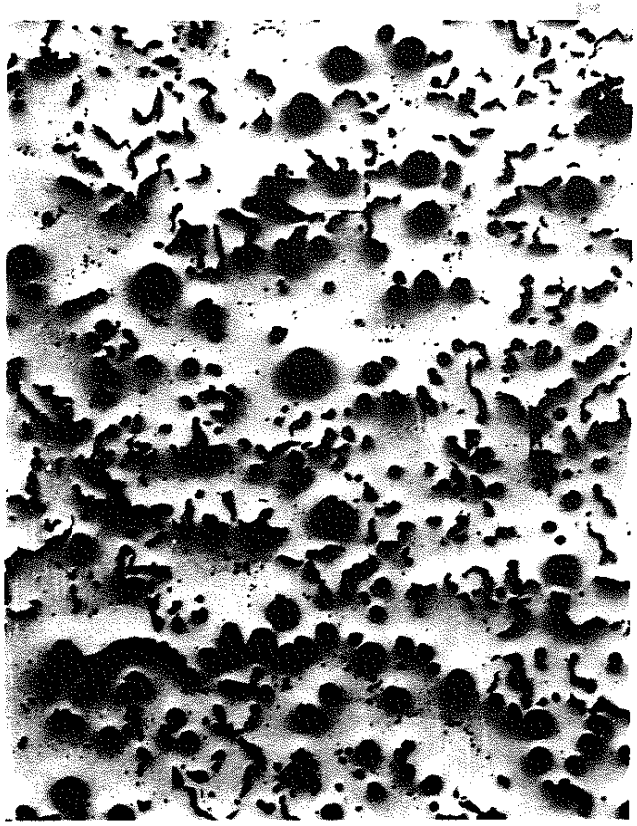

(i)

(ii)

Figure 2 Compacted Graphite Iron-CG(B)
(i) CG Form with ≈25% Nodular Graphite
(ii) Matrix Microstructure-Pearlite Etched 2% Nital

(i)

(ii)

Figure 3 Pearlitic Gray Iron
(i) Flake Form Type A, ≈60%; Type D, ≈40%; Size 4
(ii) Matrix Microstructure-Pearlite Etched 2% Nital

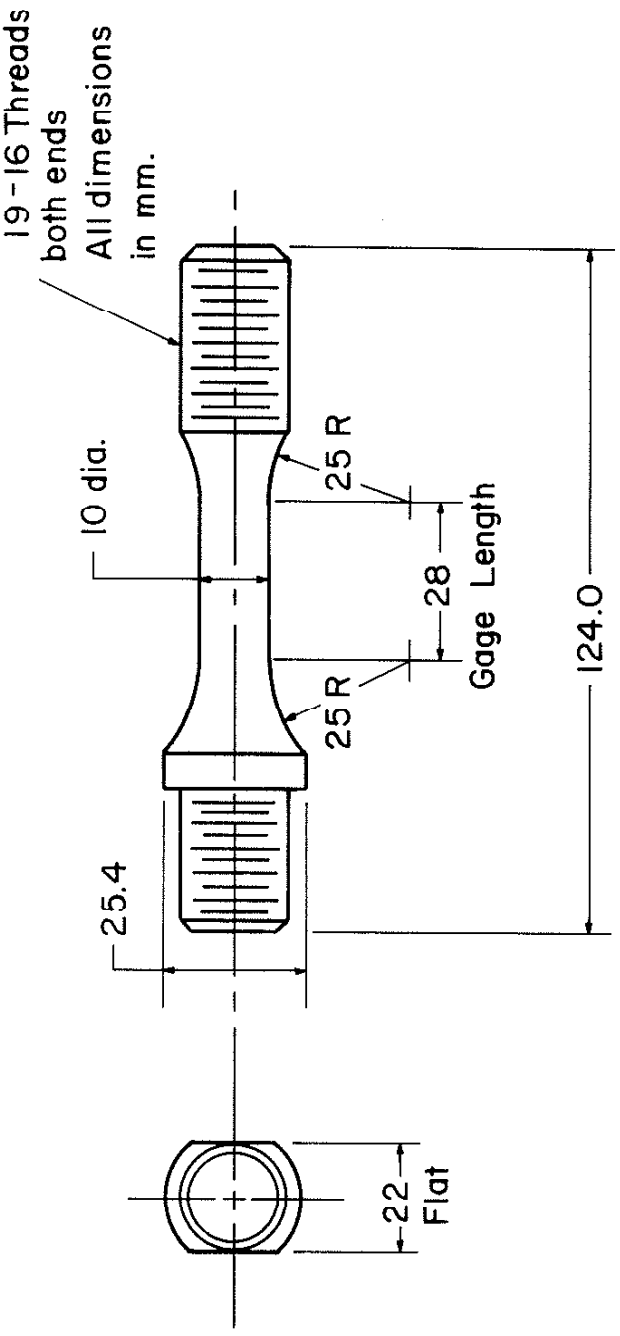

Figure 4 Laboratory Test Specimen

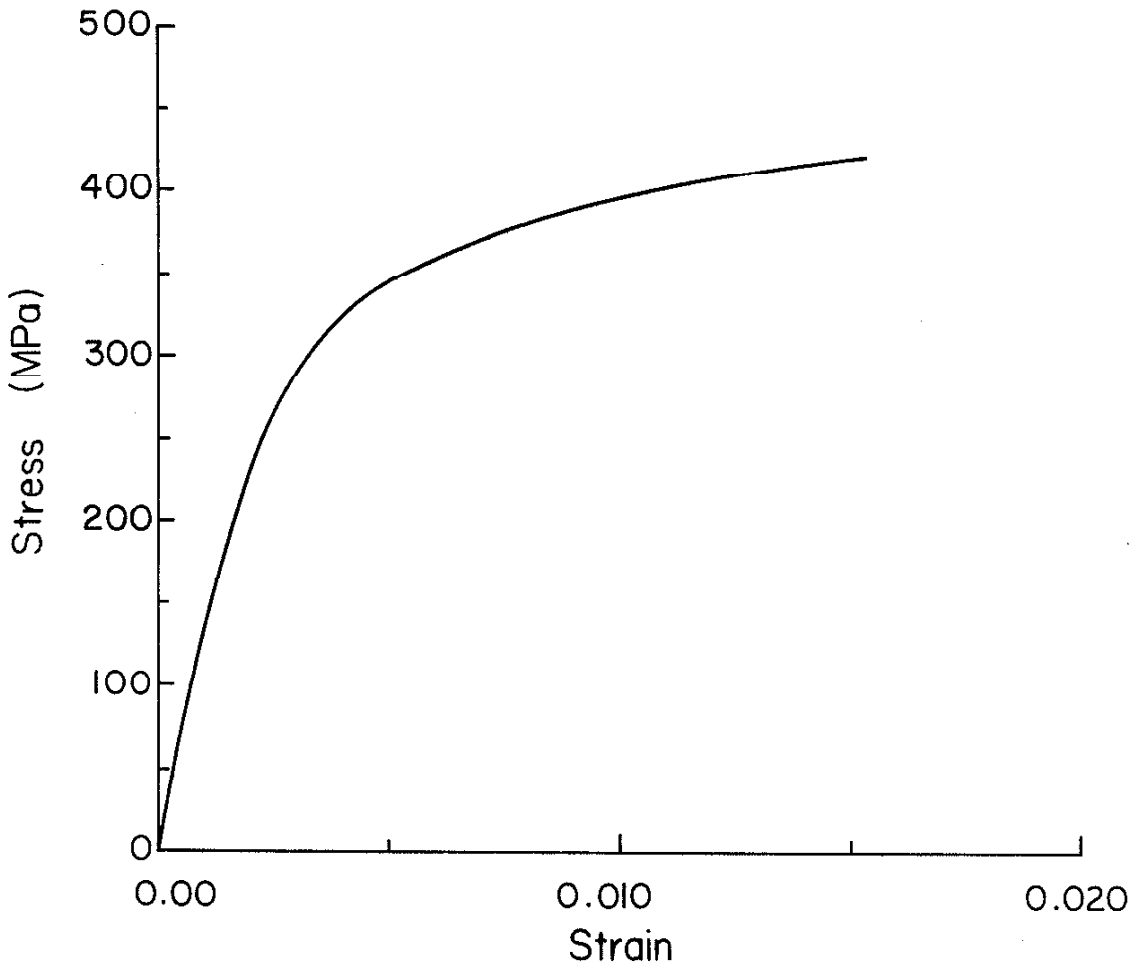

Figure 5 Monotonic Tension Stress-Strain Response of CG(A) Iron

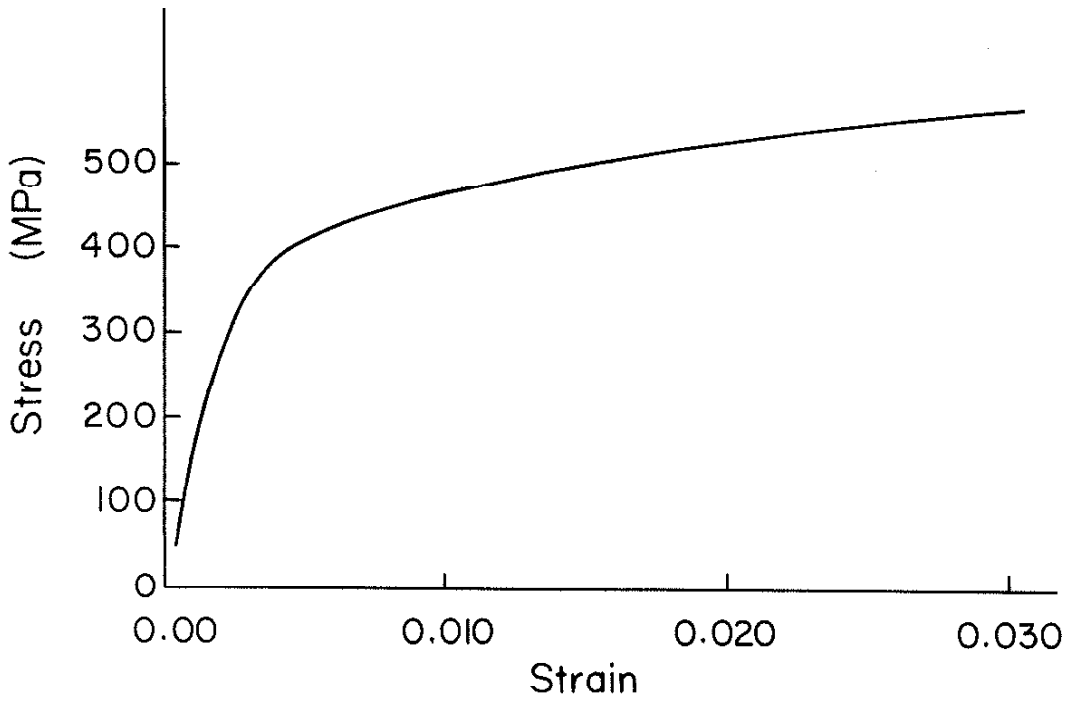

Figure 6 Monotonic Tension Stress-Strain Response of CG(B) Iron

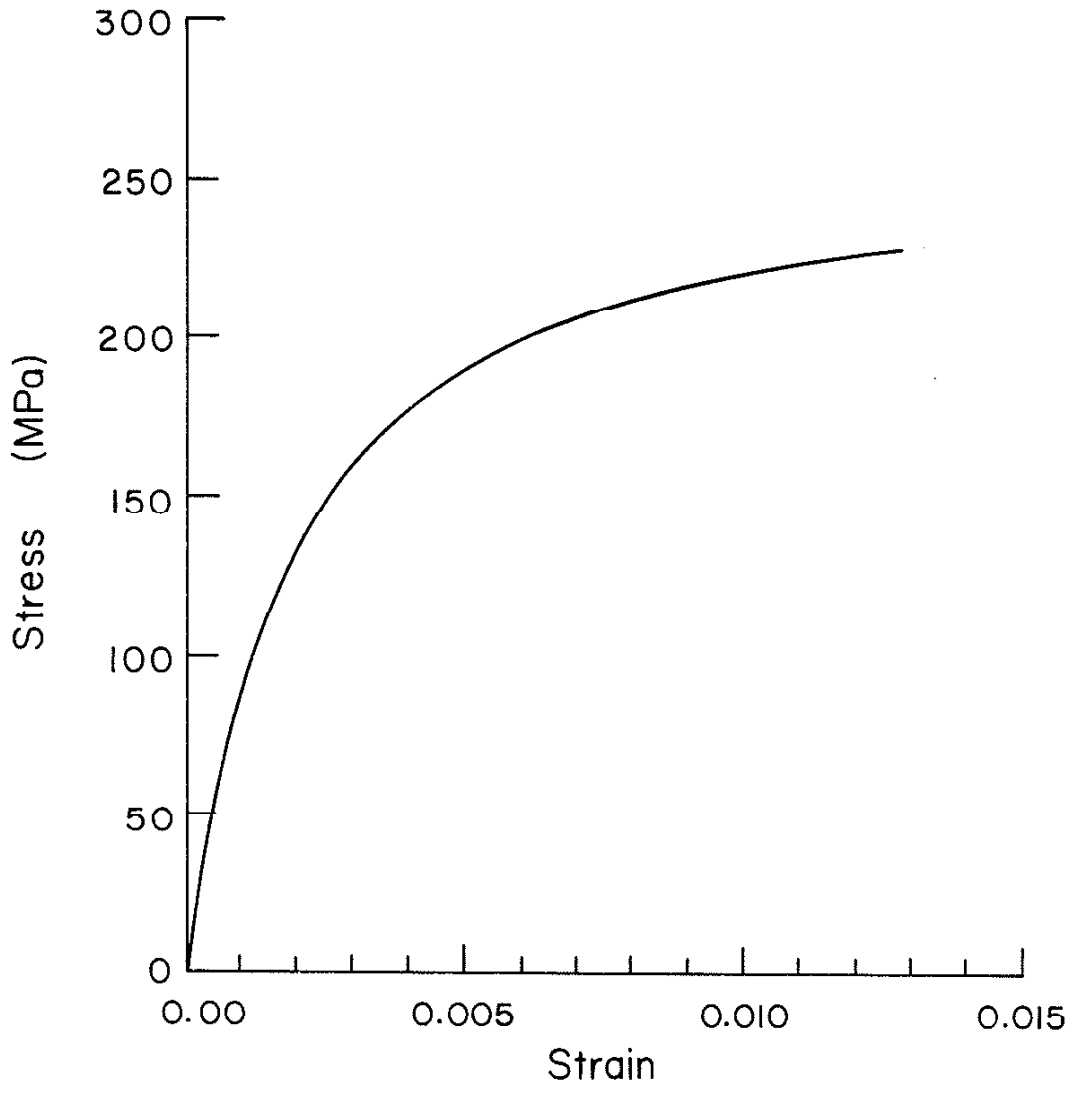

Figure 7 Monotonic Tension Stress-Strain Response of Pearlitic Gray Iron

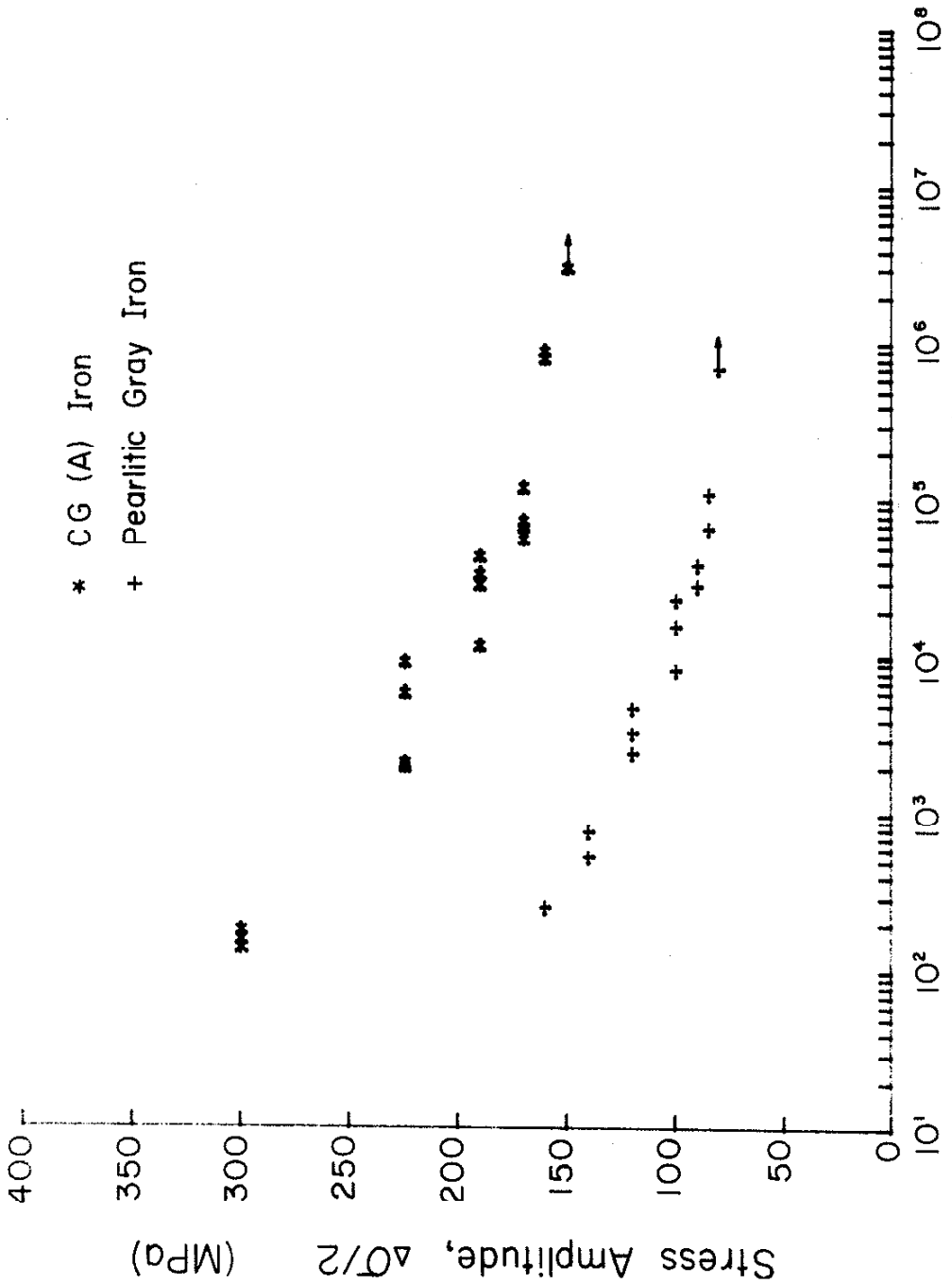

Figure 8 Stress-Life Fatigue Data for CG(A) and Pearlitic Gray Iron

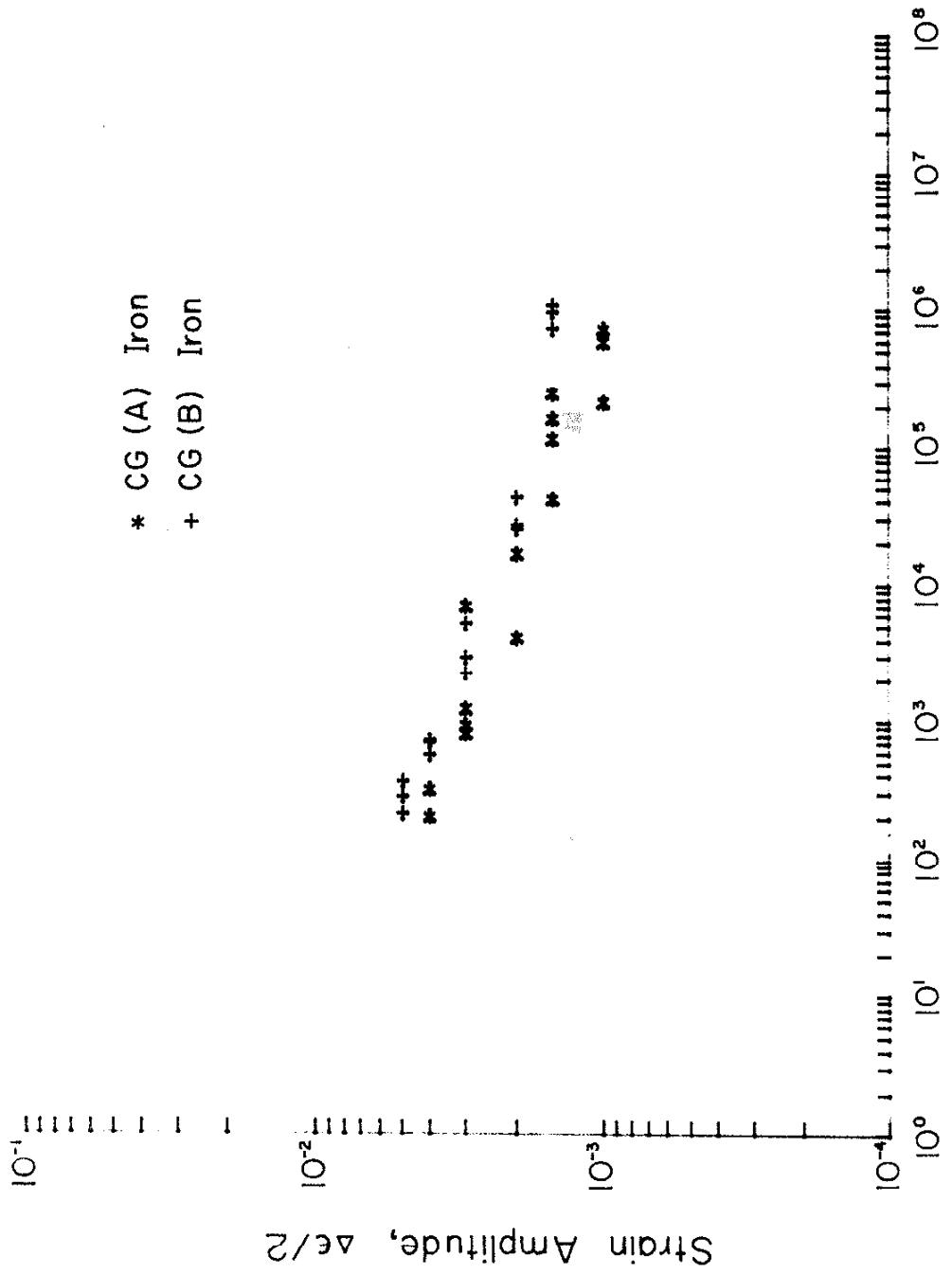

Figure 9 Strain-Life Fatigue Data for CG(A) and CG(B)

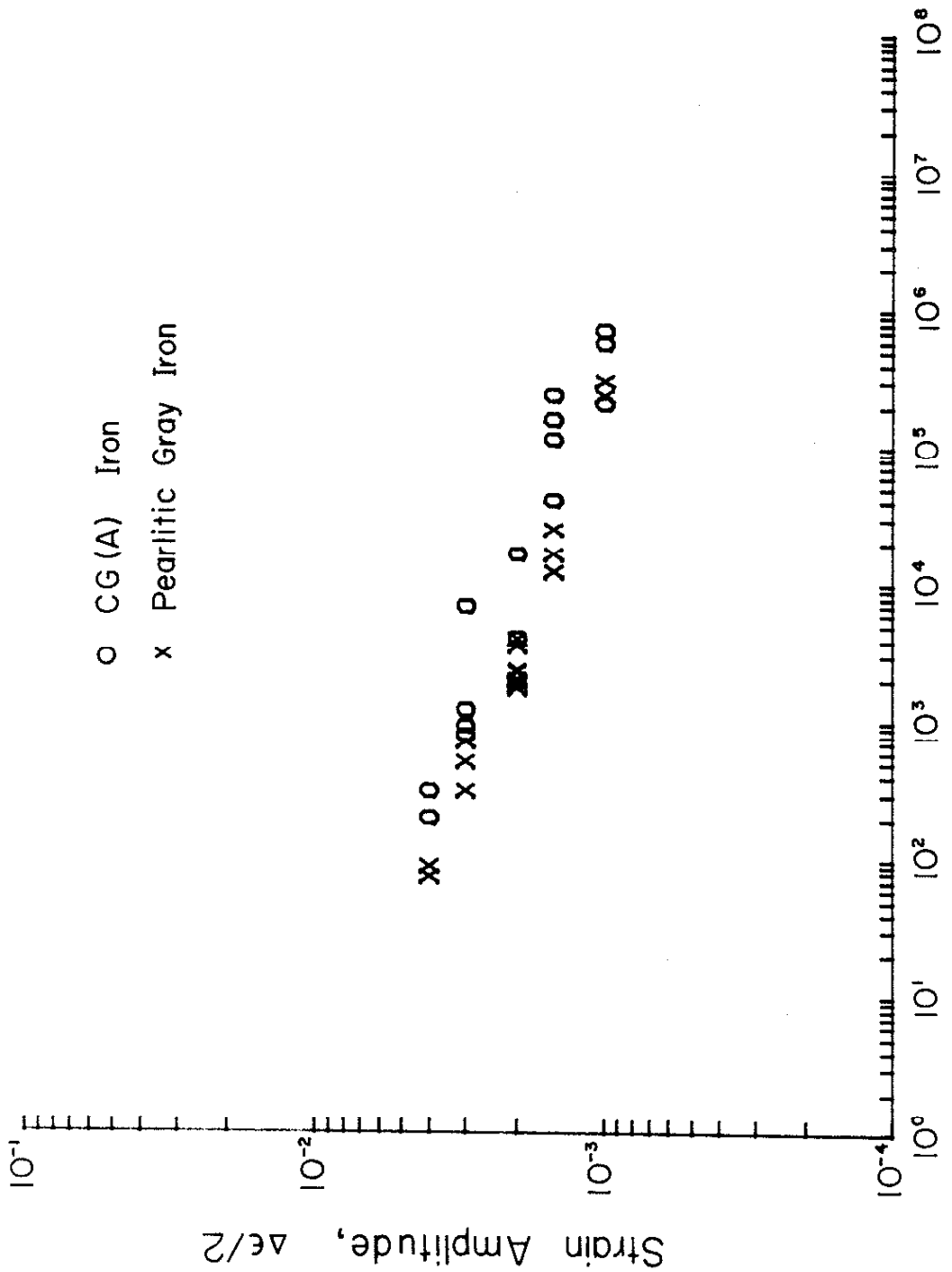

Figure 10 Strain-Life Fatigue Data for CG(A) and Pearlitic Gray Iron

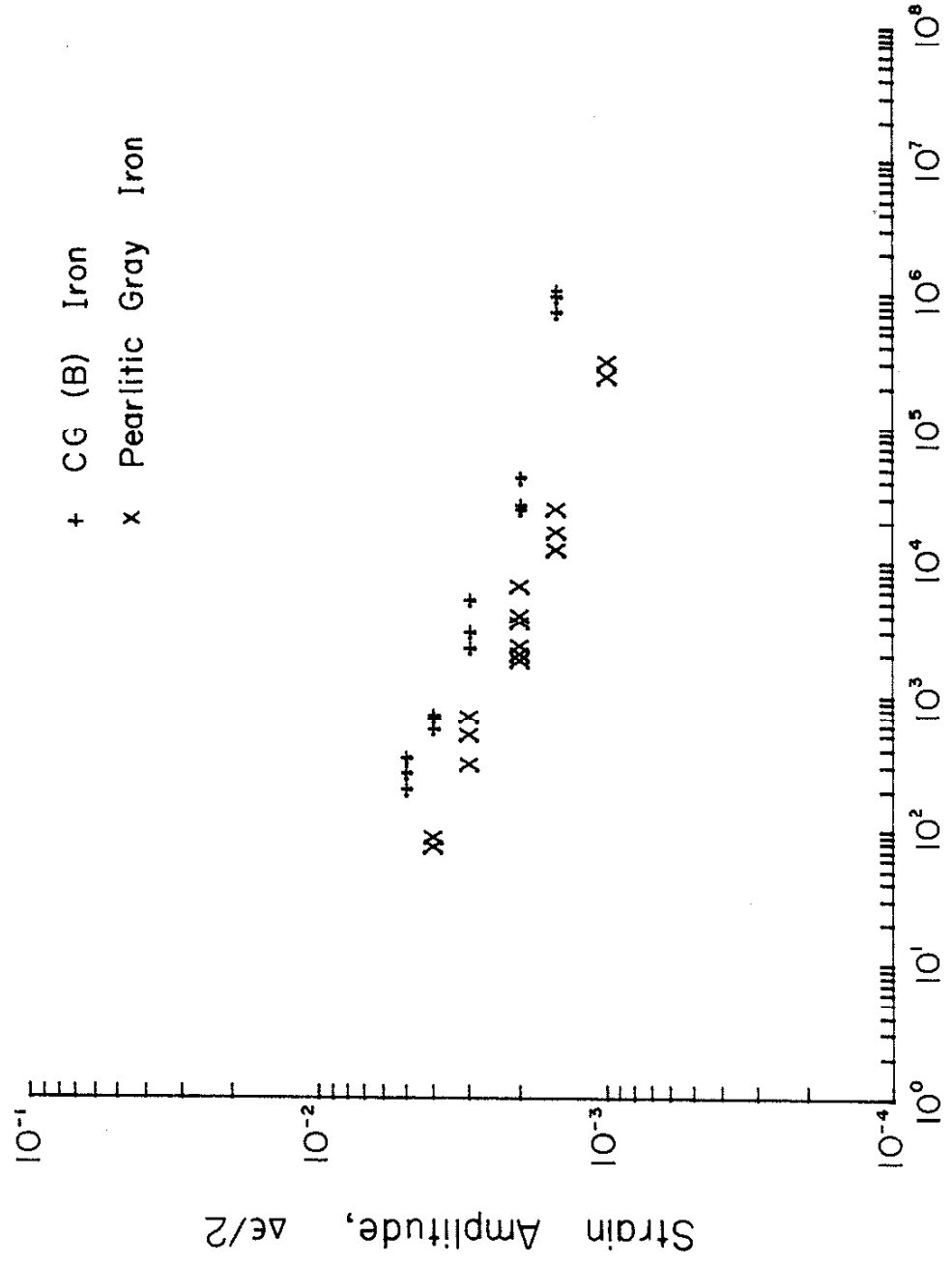

Figure 11 Strain-Life Fatigue Data for CG(B) and Pearlitic Gray Iron

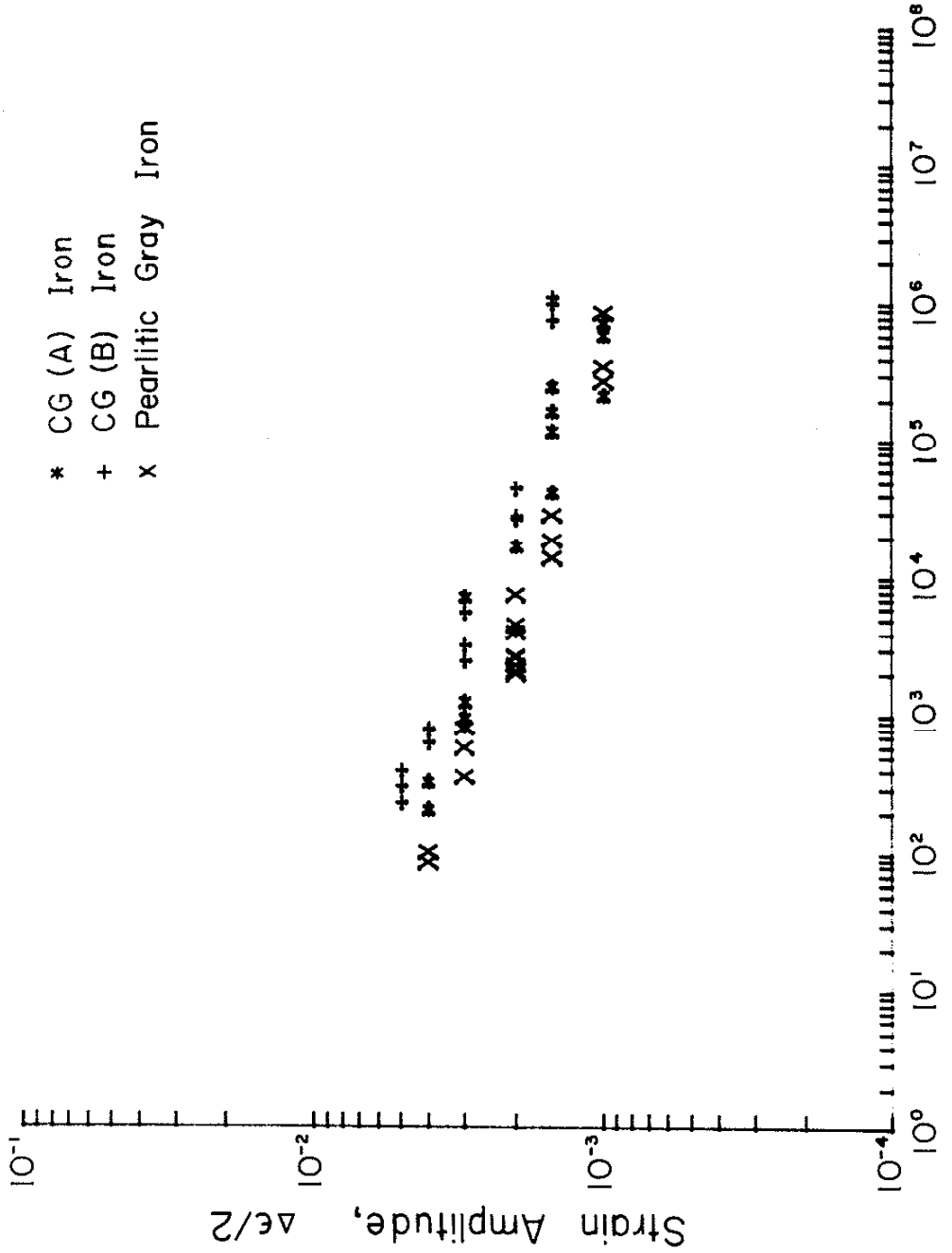

Figure 12 Strain-Life Fatigue Data for Three Irons Tested

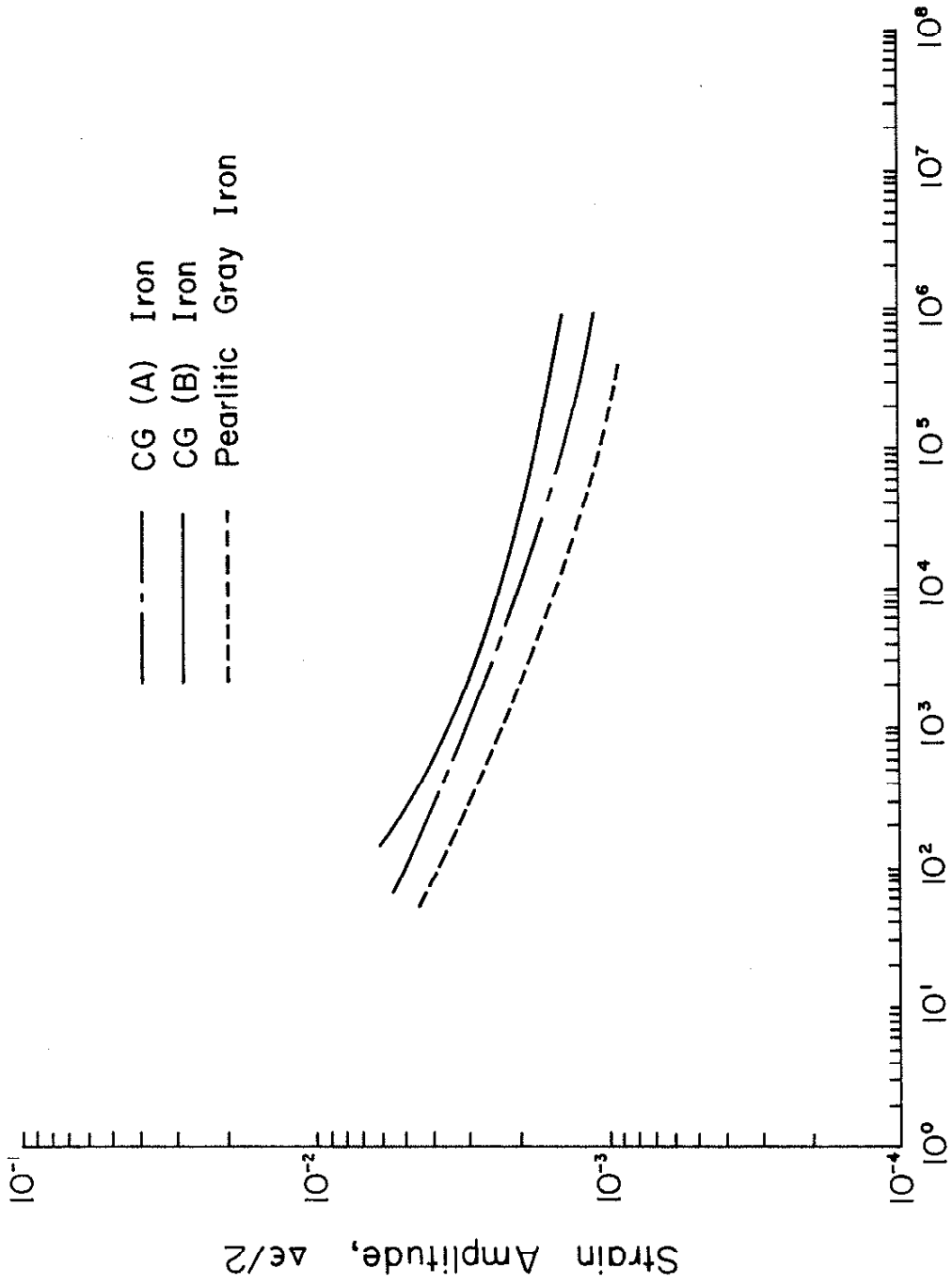

Figure 13 Strain-Life Curves for Three Irons Tested

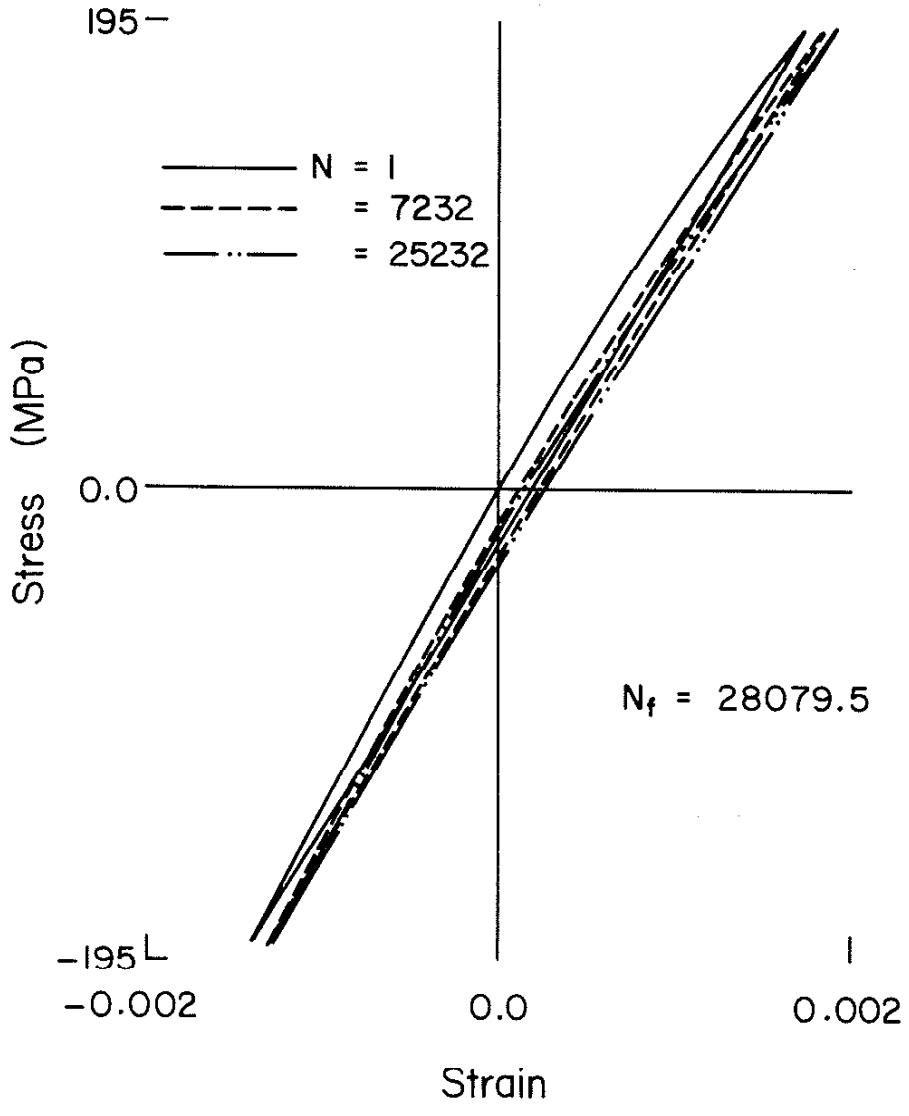

Figure 14 Hysteresis Response of CG(A) Iron; $\Delta\sigma/2$ = 190 (MPa)

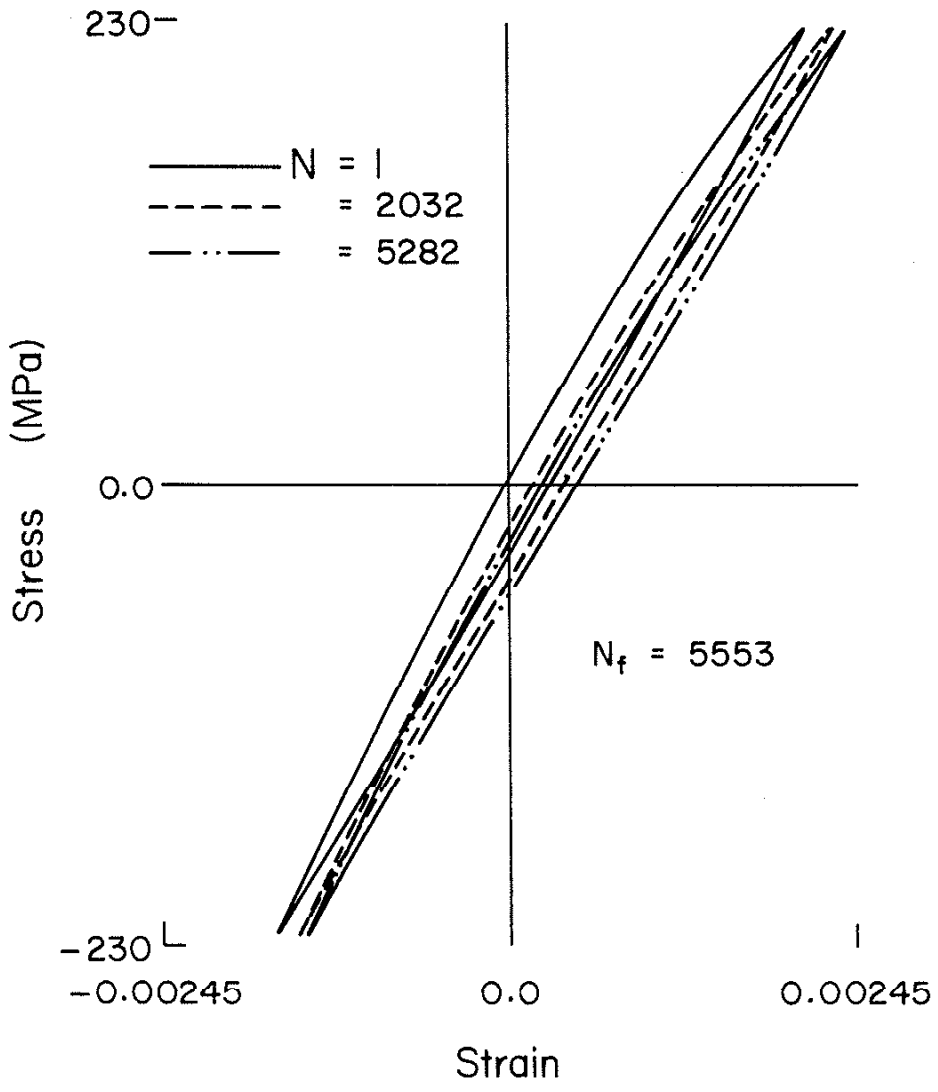

Figure 15 Hysteresis Response of CG(A) Iron; $\Delta\sigma/2$ = 225 (MPa)

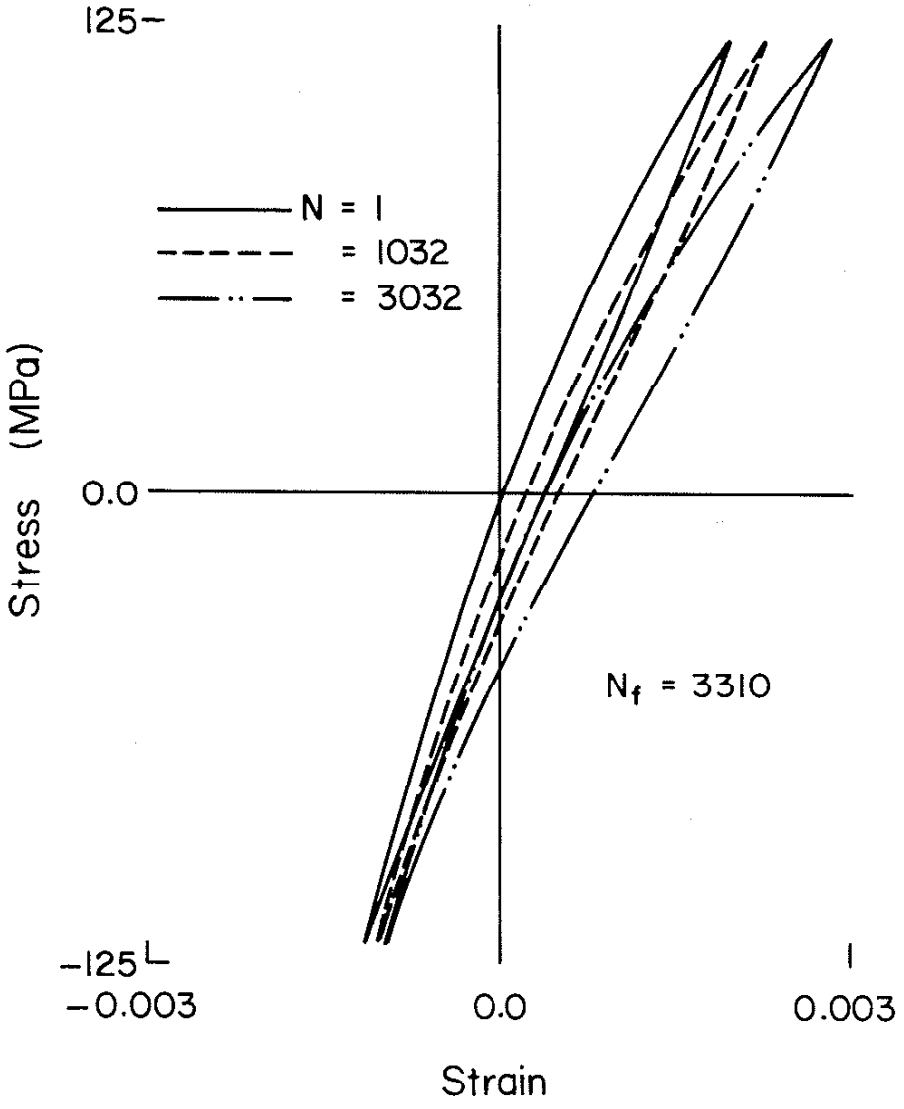

Figure 16 Hysteresis Response of Pearlitic Gray Iron; $\Delta\sigma/2$ = 120 (MPa)

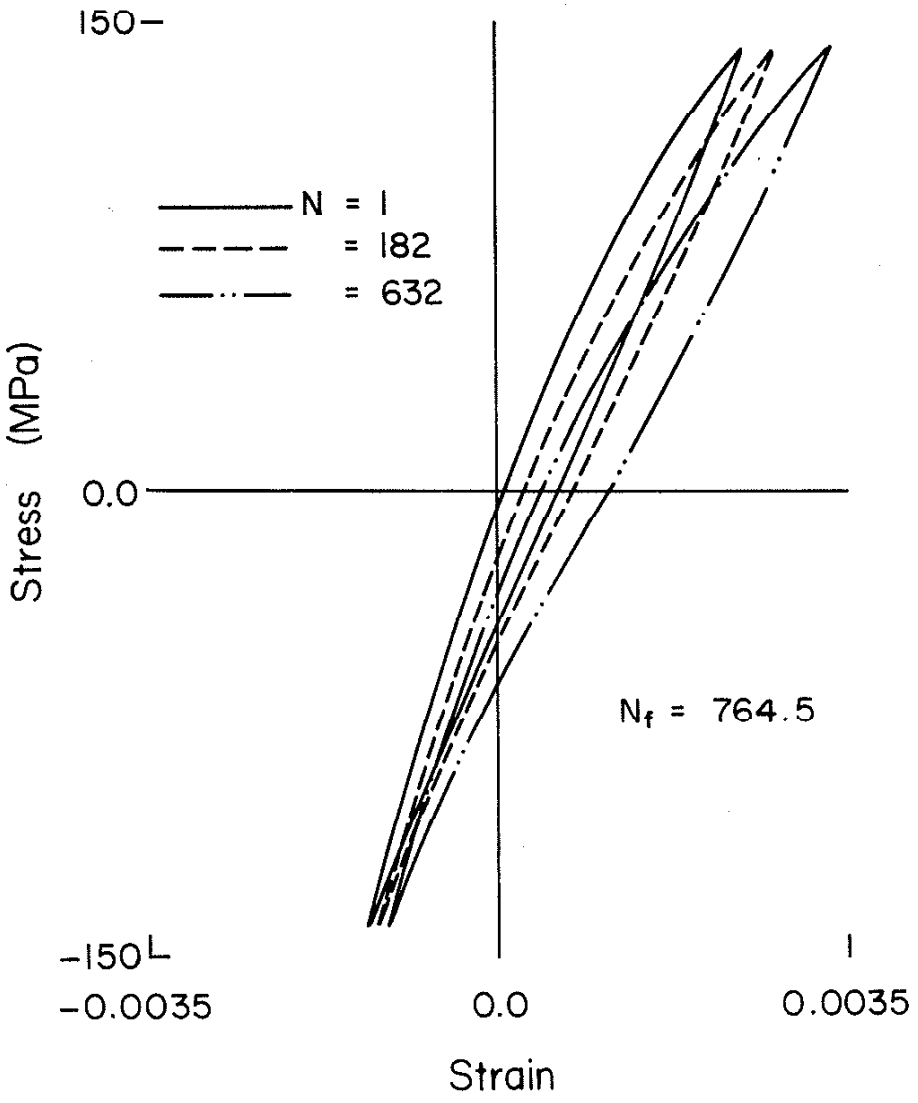

Figure 17 Hysteresis Response of Pearlitic Gray Iron; $\Delta\sigma/2$ = 140 (MPa)

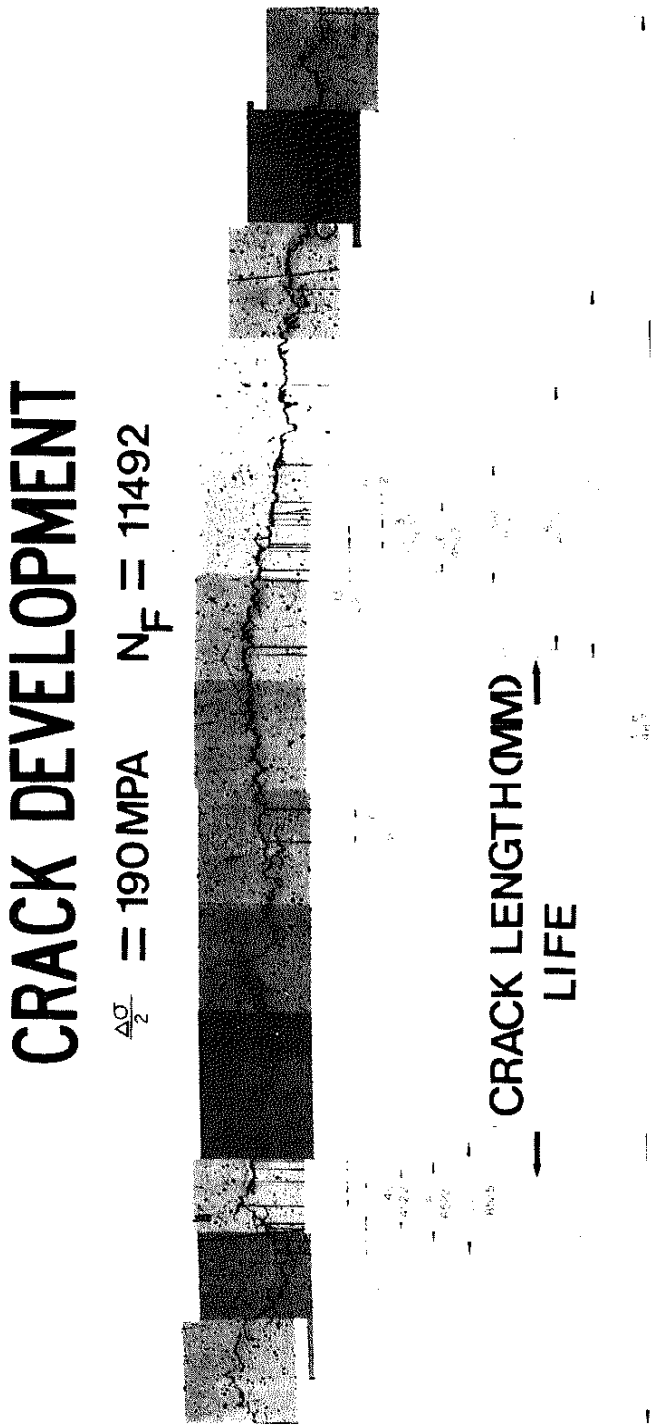

Figure 18 Crack Development in Compacted Graphite Cast Iron; $\Delta\sigma/2$ = 190 (MPa)

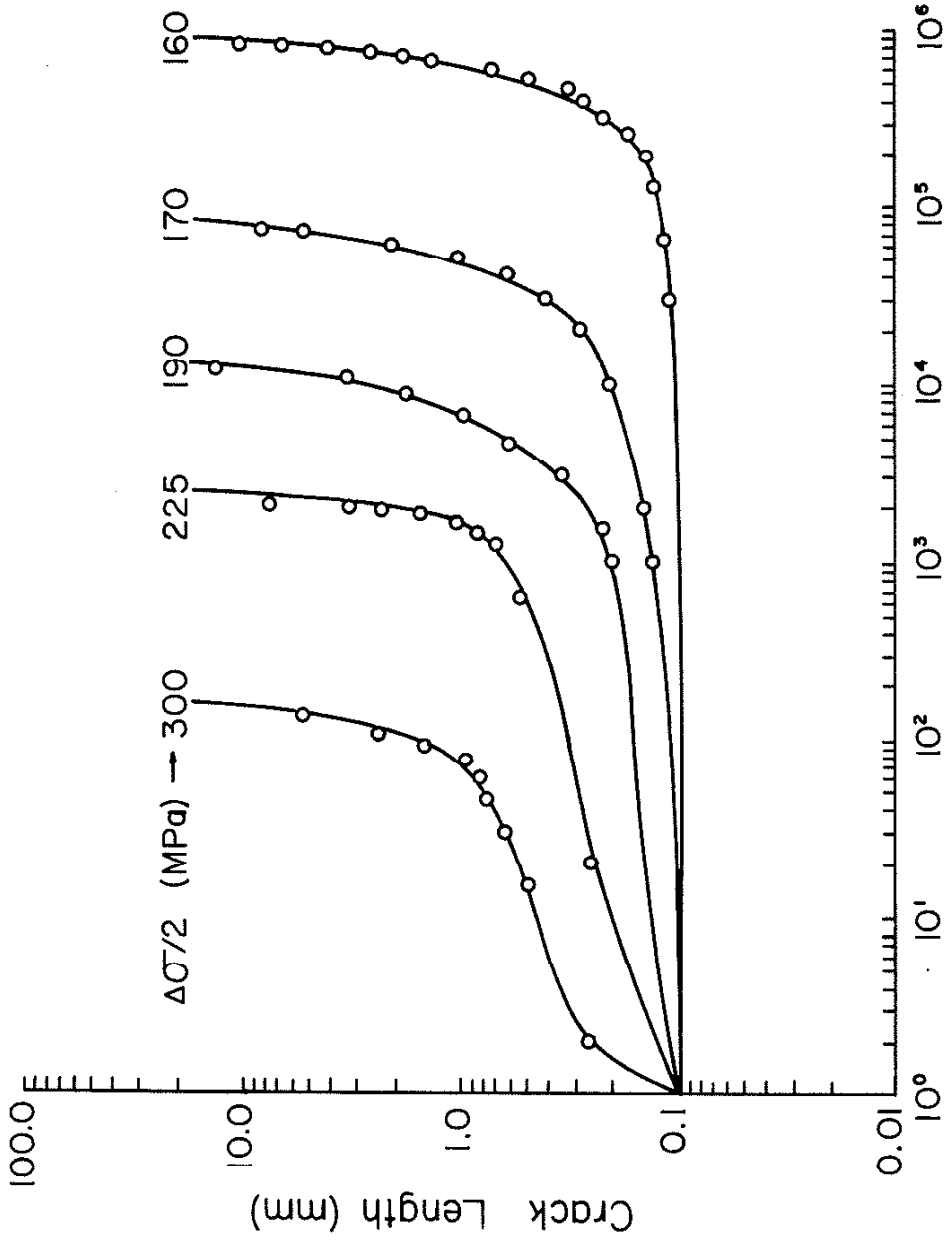

Figure 19 Crack Length versus Applied Cycles, CG(A)

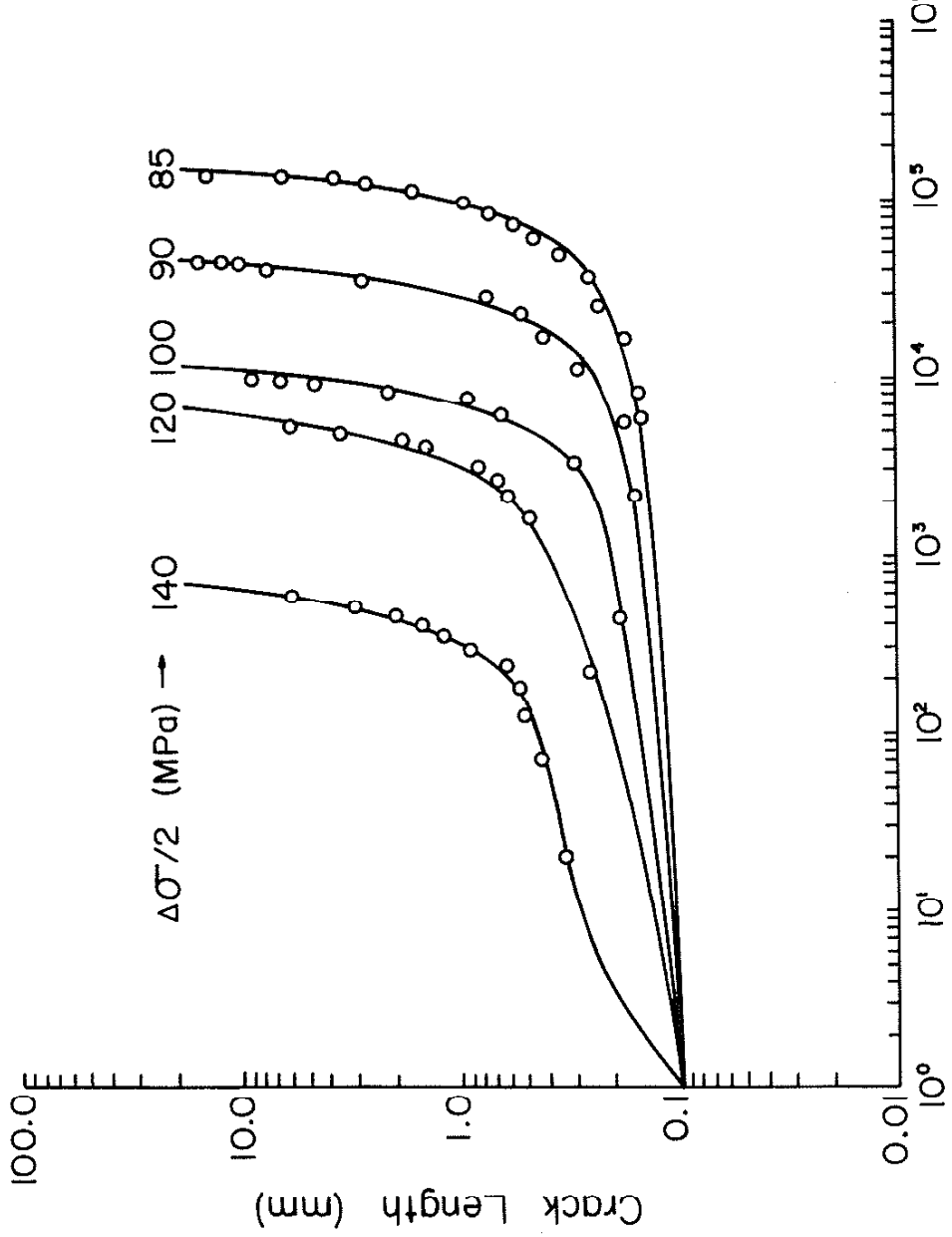

Figure 20 Crack Length versus Applied Cycles, Pearlitic Gray Iron

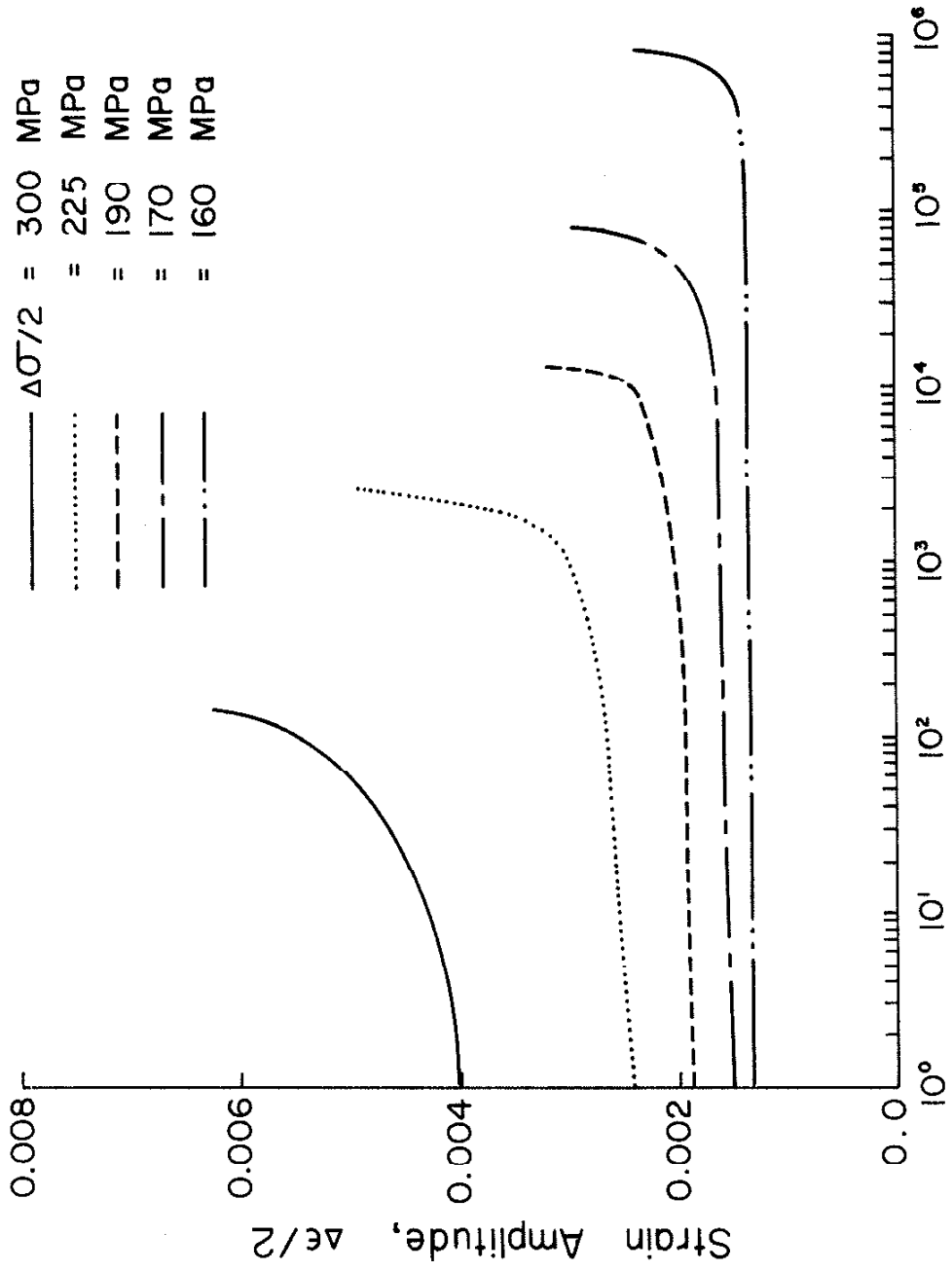

Figure 21 Strain Extension versus Applied Cycles, CG(A)

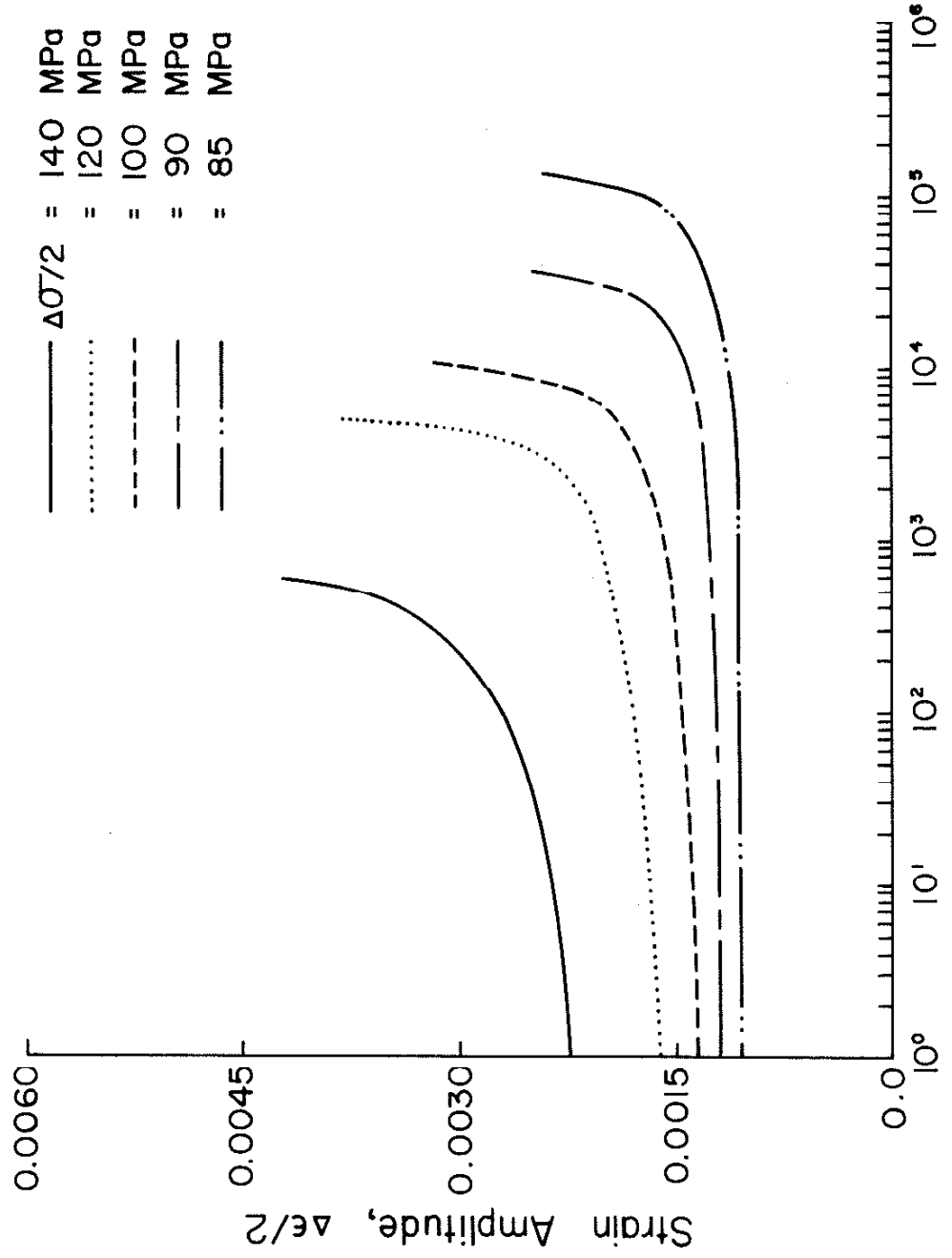

Figure 22 Strain Extension versus Applied Cycles, Pearlitic Gray Iron

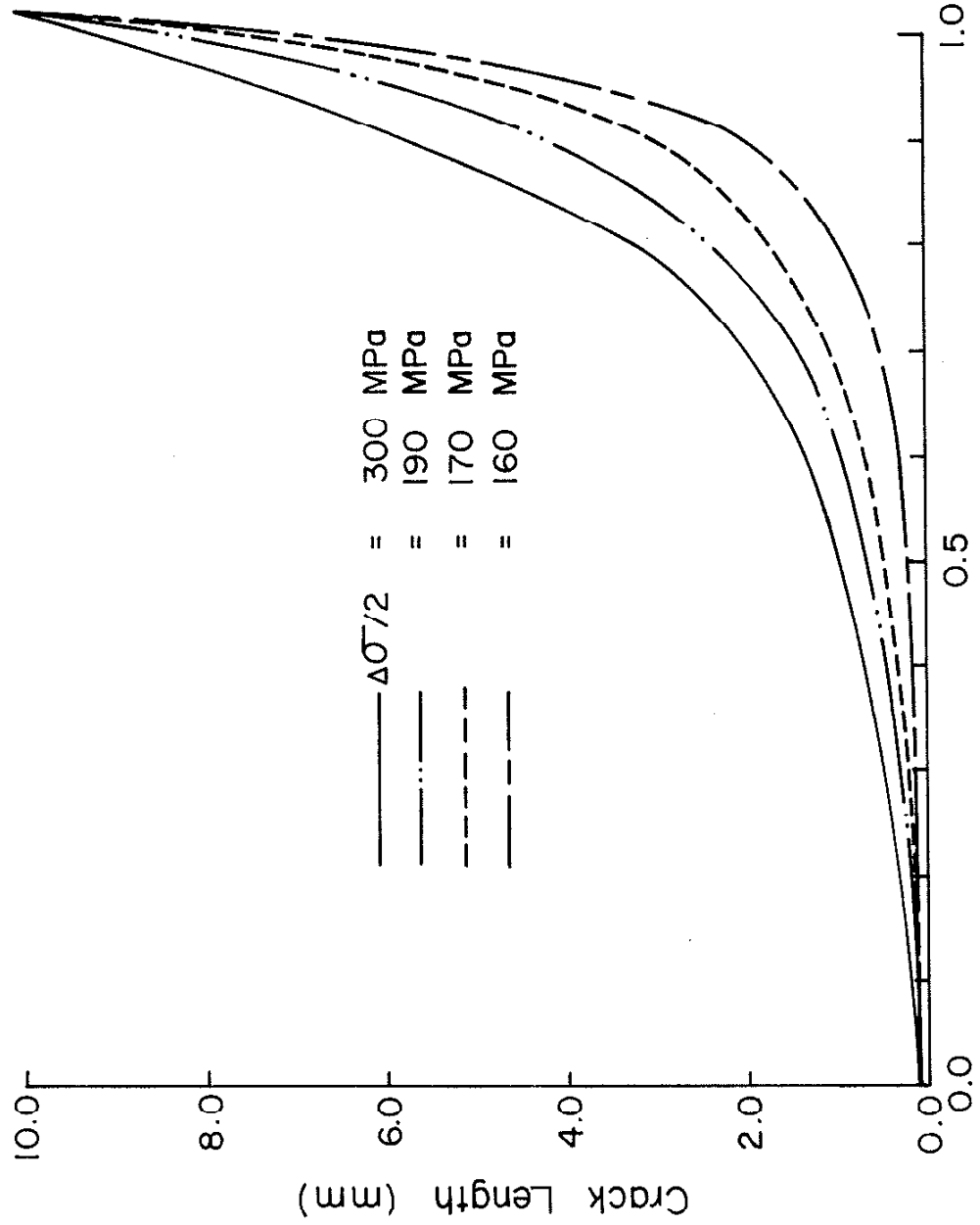

Figure 23 Crack _ength versus Applied Cycles/Cycles to Failure, CG(A)

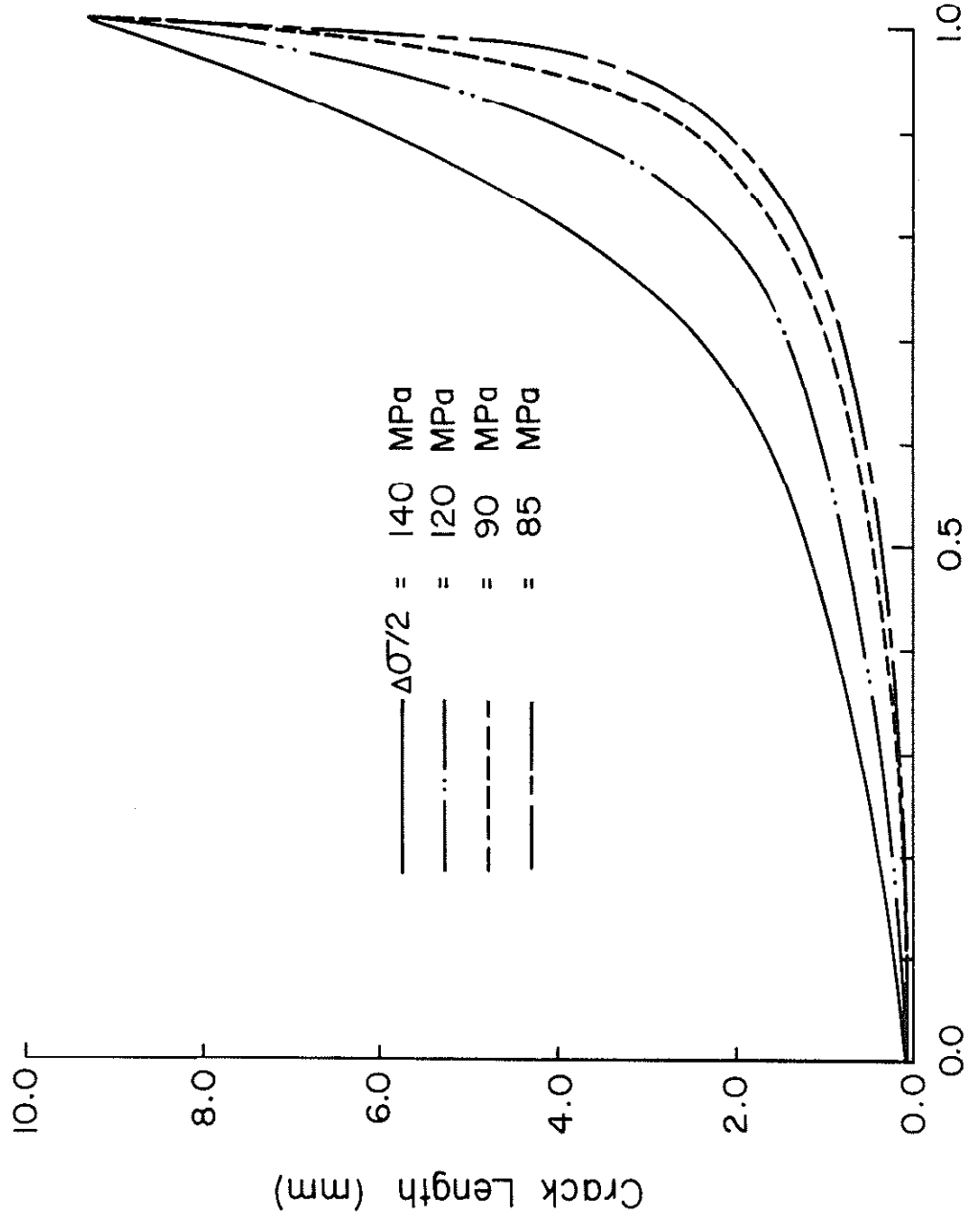

Figure 24 Crack Length versus Applied Cycles/Cycles to Failure, Gray Iron

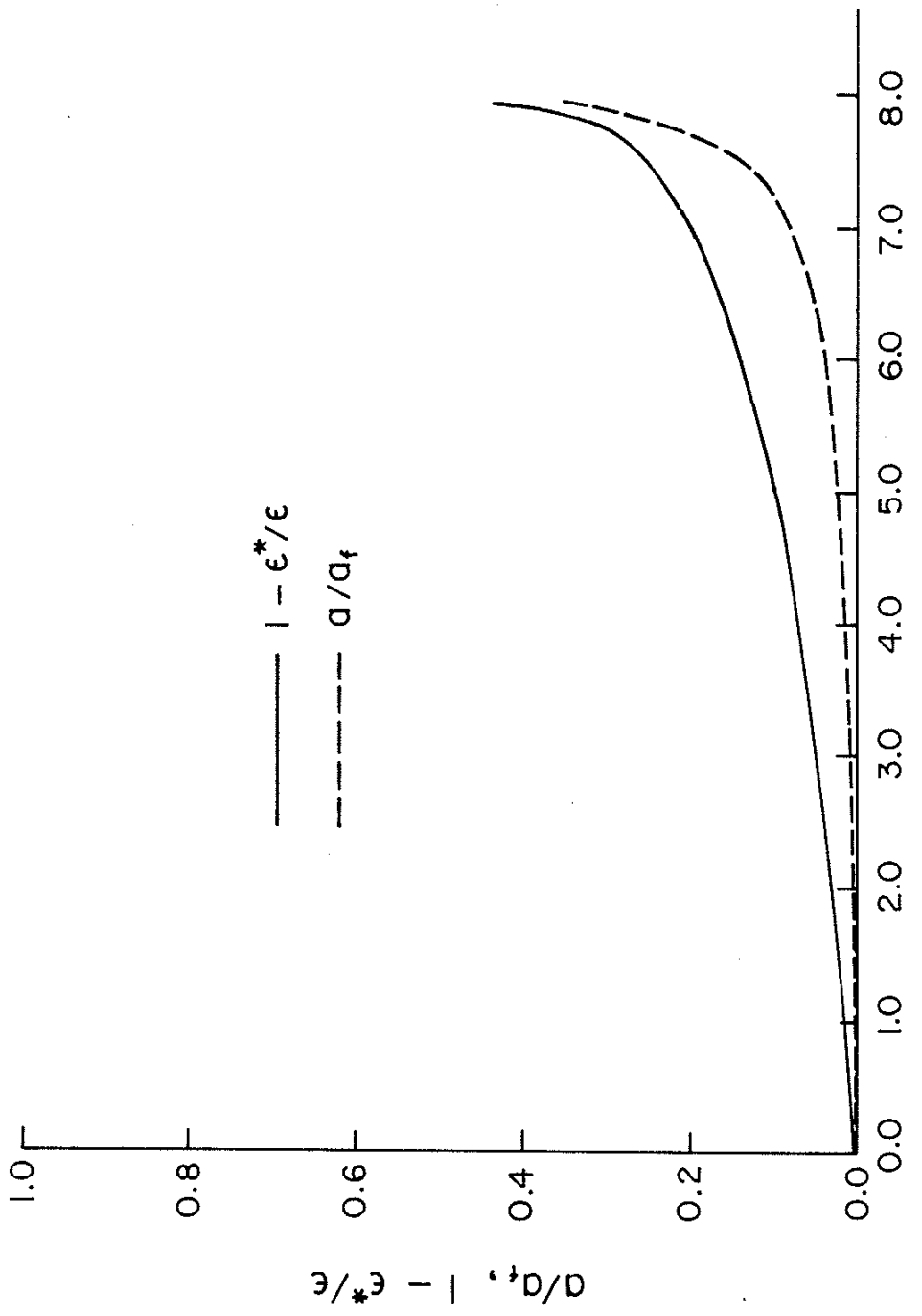

Figure 25 Normalized Strain Amplitude (Upper Curve) and Normalized Crack Length (Lower Curve) versus Applied Cycles for CG(A); $\Delta\sigma/2$ = 160 (MPa)

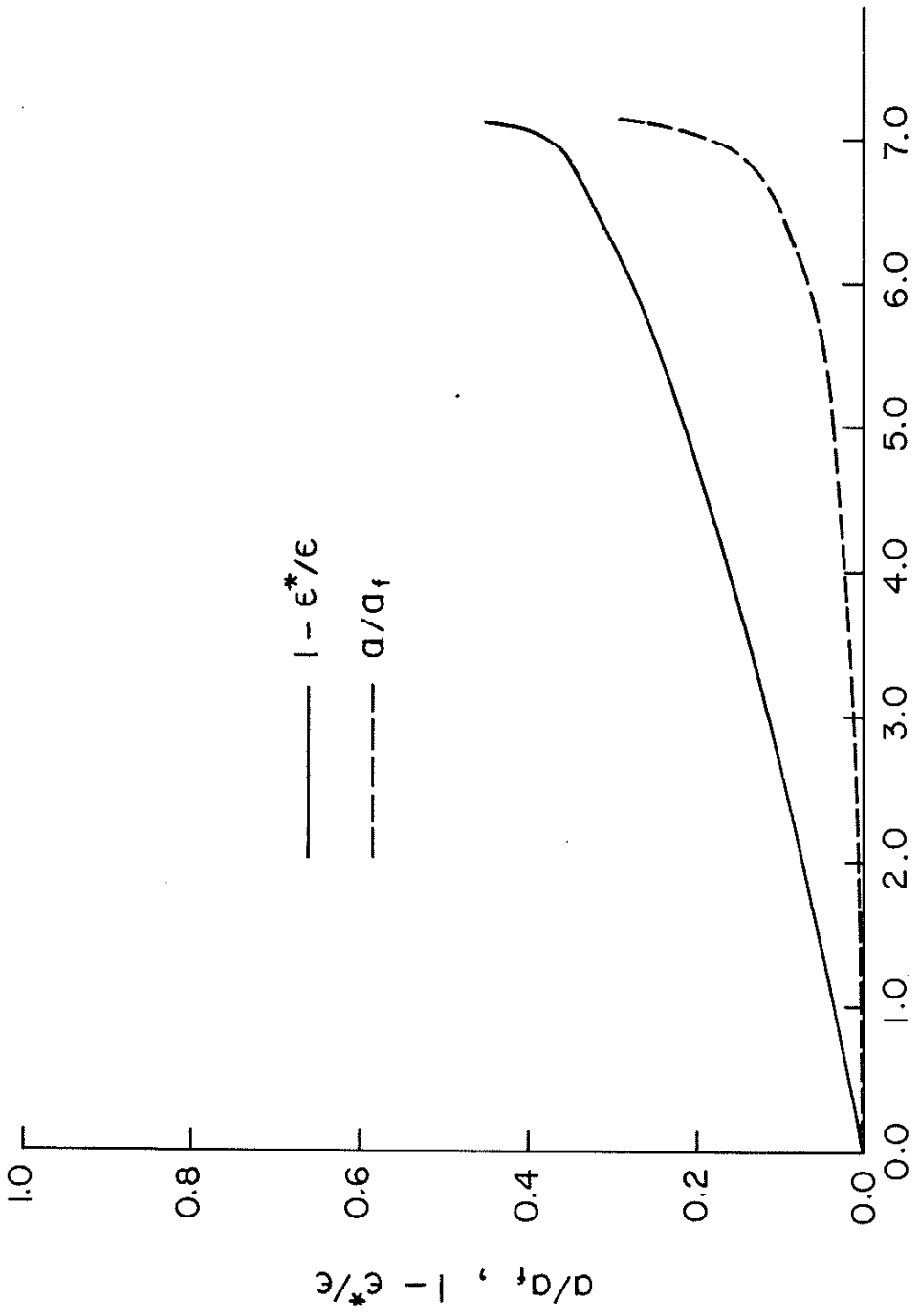

Figure 26 Normalized Strain Amplitude (Upper Curve) and Normalized Crack Length (Lower Curve) versus Applied Cycles for CG(A); $\Delta\sigma/2$ = 170 (MPa)

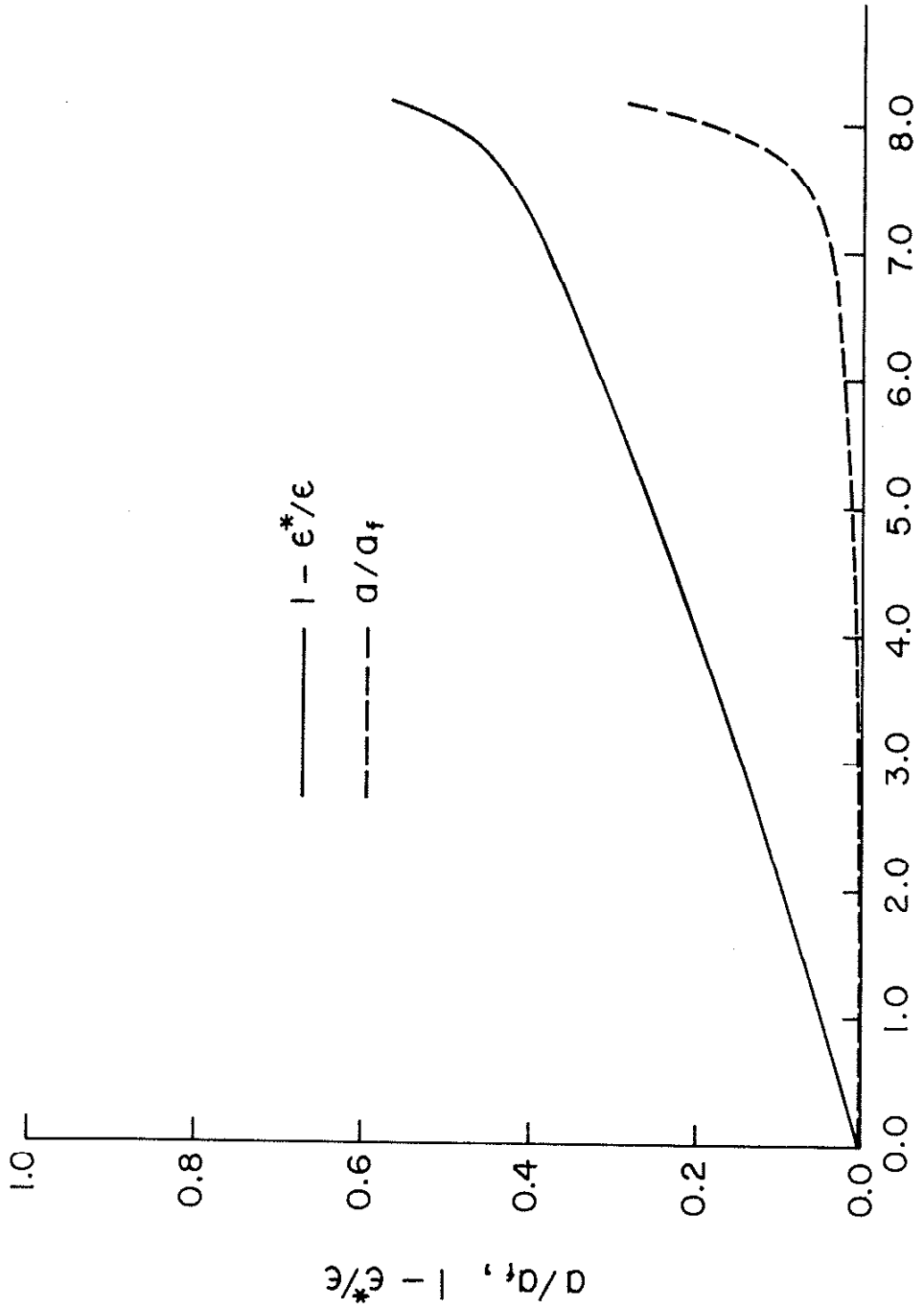

Figure 27 Normalized Strain Amplitude (Upper Curve) and Normalized Crack Length (Lower Curve) versus Applied Cycles for Gray Iron; $\Delta\sigma/2$ = 100 (MPa)

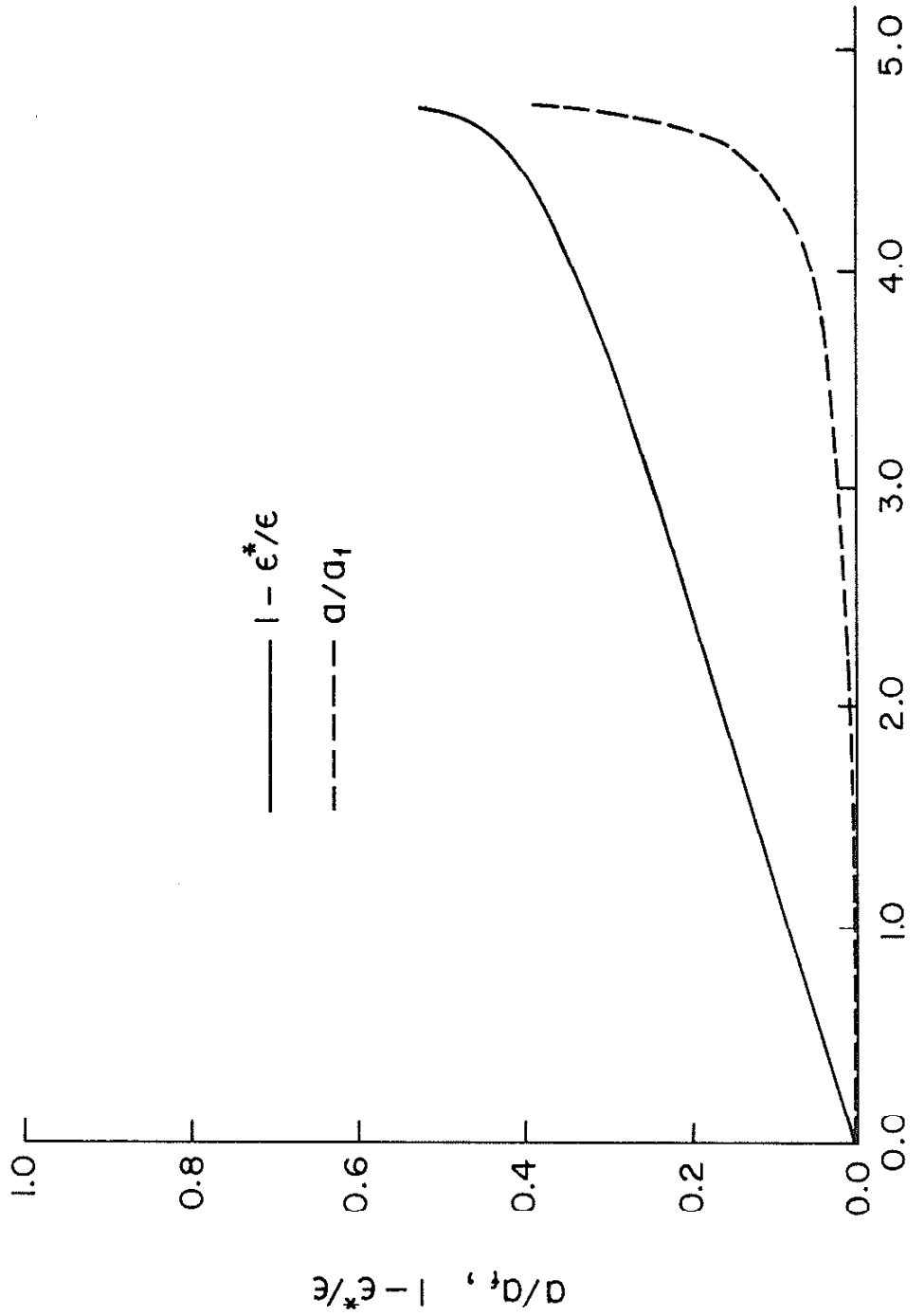

Figure 28 Normalized Strain Amplitude (Upper Curve) and Normalized Crack Length (Lower Curve) versus Applied Cycles for Gray Iron; $\Delta\sigma/2$ = 120 (MPa)

REFERENCES

1. Thum, A., and Ude, H., "Die Elastizität und die Schwingungsfestigkeit des Gusseisens," Die Giesserei, Vol. 16, 1929, pp. 547-556.

2. Ikawa, K., and Ohira, G., "Fatigue Properties of Cast Iron in Relation to Graphite Structure," American Foundry Society, Cast Metals Research Journal, Vol. 3, 1967, pp. 11-21.

3. Gilbert, G.N.J., "An Evaluation of the Stress/Strain Properties of Flake Graphite Cast Iron in Tension and Compression," Journal of the British Cast Iron Research Association, Vol. 7, 1959, pp. 745-789.

4. Gilbert, G.N.J., "The Stress/Strain Properties of Nodular Cast Irons in Tension and Compression," Journal of the British Cast Iron Research Association, Vol. 12, No. 2, 1964, pp. 170-193.

5. Gilbert, G.N.J., "Factors Relating to the Stress/Strain Properties of Cast Iron," Journal of the British Cast Iron Research Association, Vol. 6, No. 11, 1957, pp. 546-588.

6. Fash, J. W., Socie, D. F., and Russell, E. S., "Fatigue Crack Initiation and Growth in Gray Cast Iron," Proceedings of Fatigue '81, Society of Environmental Engineers, Fatigue Group Conference, Warwick University, England, March 24-27, 1981, pp. 40-51.

7. Mitchell, M. R., "Effect of Graphite Morphology, Matrix Hardness and Structure on the Fatigue Resistance of Gray Cast Iron," Society of Automotive Engineers, Inc., Report No. /50198, 1975.

8. Mitchell, M. R., "A Unified Predictive Technique for the Fatigue Resistance of Cast Ferrous-based Metals and High Hardness Wrought Steels," Society of Automotive Engineers, Inc., Report No. 790890, 1979.

9. Testin, R. A., "Characterization of the Cyclic Deformation and Fracture Behavior of Nodular Cast Iron," T&AM Report No. 371, Department of Theoretical and Applied Mechanics, University of Illinois at Urbana-Champaign, Urbana, Ill., 1973.

10. Starkey, M. S., and Irving, P. E., "The Influence of Microstructure on Fatigue Crack Initiation in Spheroidal Graphite Cast Iron," GKN Technical Report, GKN Group Technological Centre, Wolverhampton, England, 1979.

11. Morrogh, H., "Production of Nodular Graphite Structures in Gray Cast Irons," American Foundrymen's Society Transaction, Vol. 56, 1948, pp. 72-87.

12. Evans, E. R., and Dawson, J. V., "Compacted Graphite Irons and Their Production by a Single Alloy Addition," American Foundrymen's Society International Cast Metals Journal, Vol. 1, No. 2, 1976, pp. 13-18.

13. Gilbert, G.N.J., British Cast Iron Research Association, British Patent No. 1,316,438, May 9, 1973.

14. Dawson, J. V., Smith, L.W.L., and Bach, B. B., "Some Effects of Nitrogen in Cast Iron," The British Cast Iron Research Association Journal of Research and Development, Vol. 4, 1953, pp. 540-552.

15. Schelleng, R. D., British Patent No. 1,069,058, French Patent No. 1,480,448, International Nickel, Ltd., 1966.

16. Sofroni, L., Riposan, I., and Chira, I., "Some Considerations on the Crystallization Features of Cast Irons with Intermediary Shaped Graphite (Vermicular Type)," The Metallurgy of Cast Iron, Georgi Publishing Co., Saphorin, Switzerland, 1975, pp. 179-195.

17. Aleksandrov, N. N., Mil'man, B. S., Il'icheva, L. V., Andreev. V. V., and Moiseev, S. D., "Treatment of Iron with Complex REM and Yttrium Master Alloys," Russian Castings Production, July 1975, pp. 275-277.

18. Angus, H. T., Cast Iron: Physical and Engineering Properties, Second Edition, Butterworths, Inc., 1976, pp. 34-88.

19. Aleksandrov, N. N., Mil'man, B. S., Il'icheva, L. V., Osada, N. G., and Andreev, V. V., "Production and Properties of High-duty Iron with Compacted Graphite," Russian Castings Production, August 1976, pp. 319-321.

20. Palmer, K. B., "Fatigue Properties of Cast Iron, Engineering Properties and Performance of Modern Iron Castings," British Cast Iron Research Association, Birmingham, England, 1970, p. 97.

21. Riposan, I., and Sofroni, L., "Stability of the Effect of Magnesium Treatment in Compacted Graphite Cast Iron," American Foundrymen's Society International Cast Metals Journal, Vol. 3, No. 1, 1978, pp. 23-28.

22. Tucker, L. E., and Olberts, D. R., "Fatigue Properties of Gray Cast Iron," Society of Automotive Engineers, Inc., Report No. 690471, 1969.

APPENDIX

CRACK GROWTH TEST REPLICATING TECHNIQUE

The procedure for obtaining replicas of a specimen in load control mode is outlined below.

1. Test performed in load control mode.
2. Record hysteresis loop.
3. Go to zero load.
4. Record strain $\varepsilon = \varepsilon^*$ at load $P = 0$.
5. Hydraulics off.
6. Remove extensometer.
7. Apply replicating load.
8. Take replicas.
9. Return to $P = 0$.
10. Remount extensometer.
11. Set offset on extensometer with amplifier zero control to strain reading of ε^*.
12. Hydraulics on.
13. Resume test if $\varepsilon = \varepsilon^*$.